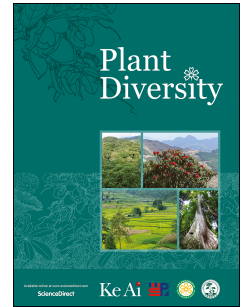


# Journal Pre-proof

Siwalik plant megafossil diversity in the Eastern Himalayas: A review

Mahasin Ali Khan, Sumana Mahato, Robert A. Spicer, Teresa E.V. Spicer, Ashif Ali, Taposhi Hazra, Subir Bera



PII: S2468-2659(22)00128-7

DOI: <https://doi.org/10.1016/j.pld.2022.12.003>

Reference: PLD 385

To appear in: *Plant Diversity*

Received Date: 31 July 2022

Revised Date: 5 December 2022

Accepted Date: 8 December 2022

Please cite this article as: Khan, M.A., Mahato, S., Spicer, R.A., Spicer, T.E.V., Ali, A., Hazra, T., Bera, S., Siwalik plant megafossil diversity in the Eastern Himalayas: A review, *Plant Diversity*, <https://doi.org/10.1016/j.pld.2022.12.003>.

This is a PDF file of an article that has undergone enhancements after acceptance, such as the addition of a cover page and metadata, and formatting for readability, but it is not yet the definitive version of record. This version will undergo additional copyediting, typesetting and review before it is published in its final form, but we are providing this version to give early visibility of the article. Please note that, during the production process, errors may be discovered which could affect the content, and all legal disclaimers that apply to the journal pertain.

© 2022 Kunming Institute of Botany, Chinese Academy of Sciences. Publishing services by Elsevier B.V. on behalf of KeAi Communications Co. Ltd.

1 **Siwalik Plant Megafossil Diversity in the Eastern Himalayas: A**

2 **Review**

3 **Mahasin Ali Khan<sup>1\*+</sup>, Sumana Mahato<sup>1+</sup>, Robert A. Spicer<sup>2,3</sup>, Teresa E. V. Spicer<sup>2</sup>, Ashif**  
4 **Ali<sup>1</sup>, Taposhi Hazra<sup>1</sup> and Subir Bera<sup>4</sup>**

5 <sup>1</sup>Palaeobotany and Palynology Laboratory, Department of Botany, Sidho-Kanho-Birsha

6 University, Ranchi Road, Purulia-723104, India

7 <sup>2</sup>CAS Key Laboratory of Tropical Forest Ecology, Xishuangbanna Tropical Botanical Garden,

8 Chinese Academy of Sciences, Mengla 666303, P.R. China

9 <sup>3</sup>School of Environment, Earth and Ecosystem Sciences, The Open University, Milton Keynes,

10 MK7 6AA, UK.

11 <sup>4</sup>Centre of Advanced Study, Department of Botany, University of Calcutta, 35, B.C. Road,

12 Kolkata-700019, India

13 **\*Corresponding author, E-mail: [khan.mahasinali@gmail.com](mailto:khan.mahasinali@gmail.com)**

14 + These authors contributed equally to this work.

15

16

1 **Siwalik plant megafossil diversity in the Eastern Himalayas: A**

2 **review**

3 **Mahasin Ali Khan<sup>1\*+</sup>, Sumana Mahato<sup>1+</sup>, Robert A. Spicer<sup>2,3</sup>, Teresa E.V. Spicer<sup>2</sup>, Ashif**

4 **Ali<sup>1</sup>, Taposhi Hazra<sup>1</sup>, Subir Bera<sup>4</sup>**

5 <sup>1</sup>Palaeobotany and Palynology Laboratory, Department of Botany, Sidho-Kanho-Birsha

6 University, Ranchi Road, Purulia 723104, India

7 <sup>2</sup>CAS Key Laboratory of Tropical Forest Ecology, Xishuangbanna Tropical Botanical Garden,

8 Chinese Academy of Sciences, Mengla 666303, P.R. China

9 <sup>3</sup>School of Environment, Earth and Ecosystem Sciences, The Open University, Milton Keynes,

10 MK7 6AA, UK

11 <sup>4</sup>Centre of Advanced Study, Department of Botany, University of Calcutta, 35, B.C. Road,

12 Kolkata 700019, India

13 **\*Corresponding author, E-mail: [khan.mahasinali@gmail.com](mailto:khan.mahasinali@gmail.com)**

14 + These authors contributed equally to this work.

15

16

17

18

19

20

21

22

## 23 **Abstract**

24 The Eastern Himalayas are renowned for their high plant diversity. To understand how this  
25 modern botanical richness formed, it is critical to investigate past plant biodiversity preserved as  
26 fossils throughout the eastern Himalayan Siwalik succession (middle Miocene–early  
27 Pleistocene). Here, we present a summary of plant diversity records that document Neogene  
28 floristic and climate changes. We do this by compiling published records of megafossil plant  
29 remains, because these offer better spatial and temporal resolution than do palynological records.  
30 Analyses of the Siwalik floral assemblages based on the distribution of the nearest living relative  
31 taxa suggest that a tropical wet evergreen forest was growing in a warm humid monsoonal  
32 climate at the deposition time. This qualitative interpretation is also corroborated by published  
33 CLAMP (Climate Leaf Analysis Multivariate Program) analyses. Here, we also reconstruct the  
34 climate by applying a new common proxy WorldClim2 calibration. This allows the detection of  
35 subtle climate differences between floral assemblages free of artefacts introduced by using  
36 different methodologies and climate calibrations. An analysis of the Siwalik floras indicates that  
37 there was a gradual change in floral composition. The lower Siwalik assemblages provide  
38 evidence of a predominance of evergreen elements. An increase in deciduous elements in the  
39 floral composition is noticed towards the close of the middle Siwalik and the beginning of the  
40 upper Siwalik formation. This change reflects a climatic difference between Miocene and Plio-  
41 Pleistocene times. This review helps us to understand under what paleoenvironmental conditions  
42 plant diversity occurred and evolved in the eastern Himalayas throughout the Cenozoic.

43

44 **Keywords:** Megafossils; Siwalik; Miocene–Pleistocene; Palaeovegetation; Palaeoenvironment;  
45 Eastern Himalayas

## 46 **1. Introduction**

47 ‘Siwalik’ sediments comprise a thick (about 7000 m) succession of Neogene predominantly  
48 freshwater coarsely bedded sandstone, siltstone, clay, and conglomeratic molassic deposits  
49 exposed along the length of the Himalayan foothills from the Potwar Plateau of Pakistan in the  
50 west to Assam in the east (Parkash et al., 1980; Bora and Shukla, 2005; Chakrabarti, 2016). They  
51 were deposited in a variety of fluvial environments, including piedmonts, outwash plains,  
52 channels, floodplains, and oxbow lakes, although some record marine influence (Taral et al.,  
53 2019; Debnath et al., 2021). They have accumulated close to sea level in a long but narrow  
54 foredeep to the south of the rising Himalayas since the middle Miocene time (Bora and Shukla,  
55 2005; Chakrabarti, 2016). The Siwalik succession is generally subdivided into three subgroups,  
56 namely the lower, middle, and upper Siwaliks, and their ages are assigned to middle Miocene,  
57 late Pliocene–early Pliocene, and late Pliocene–early Pleistocene respectively (Pilgrim, 1910,  
58 1913; Johnson et al., 1985; Ranga Rao et al., 1988; Valdiya, 2002). During the latest phase of the  
59 rise of the Himalayas, in Pleistocene to Recent times, ‘Siwalik’ sediments were uplifted, folded,  
60 and faulted to form a continuous mountain range of relatively low height ranging from  
61 1000–1200 m a.s.l., 2400 km in length and 20–25 km in width. From west to east along their  
62 length the Siwaliks have been divided into seven sectors: Jammu, Himachal, Uttarakhand, Nepal,  
63 Darjeeling, Bhutan, and the Southeastern Himalaya, often referred to in the literature as the  
64 Southeastern Himalaya (Karunakaran and Ranga Rao, 1976; Ranga Rao et al., 1979). Compared  
65 to their outcrops in the western and central Himalayas, the eastern Himalayan Siwaliks occur as a  
66 thinner and discontinuous belt. The Darjeeling, Bhutan, and Southeastern Himalaya Siwalik  
67 sectors of the eastern Himalayas are the focus of the present review.

68           Although a rich vertebrate fauna has been reported from eastern Himalayan Siwalik  
69 sediments (Medlicott, 1865; Pilgrim, 1910, 1913; Singh, 1975, 1983; Acharyya et al., 1987),  
70 which has helped in establishing the stratigraphy, classification, and depositional environments  
71 of the Siwalik Group of rocks, comparatively little systematic work has been carried out on the  
72 plant fossils entombed in these beds. Here, we explore the floral composition within the different  
73 units of the Siwalik succession in the eastern Himalayan sectors and trace how the climate and  
74 floras have changed through time from the middle Miocene through the Pleistocene to the  
75 present using a common proxy framework that allows direct climatic comparison between fossil  
76 sites free of artefacts that might otherwise be introduced by using a range of proxies differently  
77 calibrated.

78           The Siwalik floras offer considerable potential for studies of Neogene vegetation vis-à-vis  
79 climate change, including monsoon signatures, elevation changes within the Himalayan and  
80 Tibetan region, and plant biogeography since the middle Miocene (Prasad, 2008; Khan et al.,  
81 2014a, 2019a). The recovered fossil floras from the different eastern Siwalik sectors comprise  
82 mainly leaves of woody dicot angiosperms (Mehrotra et al., 1999; Prasad et al., 1999, 2004;  
83 Prasad and Tripathi, 2000; Prasad, 2008; Khan et al., 2014a; Srivastava et al., 2018). Here, we  
84 review fossil floras recovered from the Darjeeling, Bhutan, and Southeastern Himalaya Siwalik  
85 sectors of the eastern Himalayas and reconstruct the climate by applying a new common proxy  
86 and calibration to all the currently available eastern Siwalik fossil floras. The use of a common  
87 proxy with the same calibration has been lacking thus far as different authors tend to apply  
88 different methodologies and the methodologies themselves have evolved over time. This mix of  
89 approaches means detection and quantification of subtle changes in climate over time is hard to

90 achieve and ambiguous at best. By using a common analytical framework, we provide insights  
91 into the monsoon evolution during Siwalik depositional period in the eastern Himalayas.

92 In the present assessment, we compile all palaeobotanical plant data from published  
93 literature to document plant diversity in the eastern Himalayas throughout the Siwalik  
94 succession. We consider only fossil taxa represented by megafossils (leaves, wood, fruits,  
95 fruiting calyx, and seeds). Potential megafossils, especially leaves, cannot travel far from their  
96 point of origin before fossilization and remain identifiable (Ferguson, 1985; Spicer and Wolfe,  
97 1987; Spicer, 1991) and are destroyed when the sediments hosting them are reworked. Pollen  
98 and spores (microfossils), however, can travel long distances up and down the slope prior to final  
99 burial and still appear pristine, and can be reworked many times. Moreover, they often cannot be  
100 identified to a fine enough taxonomic resolution using only a light microscope (Ferguson et al.,  
101 2007). By focusing on megafossils we ensure that we are reconstructing vegetation local to the  
102 fossil site, and so potentially are able to detect fine-scale changes in space and time.

103 We first briefly introduce the present-day floristic composition in the eastern Himalayas,  
104 then present known fossil families, genera, and species to depict the diversity of Siwalik plants  
105 and ecosystems, and then analyze the inferred floristic characters and changes. We also  
106 summarize the Siwalik climate evolution in the eastern Himalayas. The present review aims to  
107 facilitate access to the rich Siwalik palaeobotanical record of the eastern Himalayas. We also re-  
108 examine the eastern Himalayan Siwalik Mio-Pleistocene climate and introduce new quantitative  
109 proxy palae-humidity measurements in order to characterize better the eastern Himalayan  
110 environment during a critical time of Himalayan uplift and associated evolution (Ding et al.,  
111 2017; Bhatia et al., 2021, 2022).

112

## 113 2. Geological setting

114 Pilgrim (1913) divided the Siwalik succession into three units, namely the lower (middle  
115 Miocene), middle (late Miocene to early Pliocene), and upper (late Pliocene to early  
116 Pleistocene). The Siwalik sediments are characterized by alternating sandstone and mudstone  
117 facies, with the finer sediments very often containing abundant biota (Chakrabarti, 2016). In  
118 general Siwalik sediments exhibit a coarsening trend over time, but even the youngest units  
119 contain fine-grained beds that are fossiliferous. Here, we represent a generalized  
120 lithostratigraphy of the Siwalik sediments exposed in the eastern Himalayas (Table 1; Figs. 1 and  
121 2). In the Darjeeling area, this is based on Ganguly and Rao (1970), Acharya (1994), and Taral et  
122 al. (2017); in Bhutan, we refer to Coutand et al. (2016), while in the Southeastern Himalaya we  
123 rely on Anand-Prakesh and Singh (2000) and Singh (2007). The ages of the sedimentary  
124 succession in different Siwalik sectors of the eastern Himalayas have been quantified by means  
125 of magnetostratigraphy (Chirouze et al., 2012, Coutand et al., 2016). Magnetostratigraphic  
126 correlations indicate that the Bhutan Siwalik Group was deposited during the latest Miocene and  
127 the Pleistocene, between ~7 million years ago (Ma) and ~1 Ma, and that the boundary between  
128 lower and middle Siwaliks can be dated to ~6 Ma, the middle to upper Siwalik to 3.8 Ma, and the  
129 top of the section as ~1 Ma (Coutand et al., 2016). In the Southeastern Himalaya, the Siwalik  
130 Group was deposited between 13 and 2.5 Ma, with the transition between the lower and middle  
131 Siwaliks dated at about 10.5 Ma and the middle to upper Siwalik transition at 2.6 Ma (Chirouze  
132 et al., 2012). The boundary age differences exhibited among the different parts of the eastern  
133 Himalayas could be due to temporal and locational changes in the various loci of deposition as  
134 well as local erosion events.

135



### 136 **3. Modern floristic composition of the eastern Himalayas**

137 To contextualize megafossil records from the eastern Himalayas, it is useful to consider the  
138 rich and diverse modern flora of the region. At elevations similar to those inferred for the source  
139 vegetation of the Siwalik fossil assemblages, modern vegetation close to the fossil localities in  
140 the eastern Himalayas is characterized as warm humid tropical (Champion and Seth, 1968;  
141 Biswas et al., 1976; Grierson and Long, 1983; 1996; Kaul and Haridasan, 1987; Hazra et al.,  
142 1996; Baishya et al., 2001).

143 The eastern Himalayas are considered ‘crisis ecoregions’ and ‘biodiversity hotspots’  
144 (Brooks et al., 2006). This region is also a meeting ground for the Indo-Malayan, Palearctic, and  
145 Sino-Japanese biogeographical realms, and has diverse biota as well as diverse ecological and  
146 elevational gradients (CEPF, 2005, 2007). The complex topography and extreme elevational  
147 gradients from less than 300 m (tropical lowlands) to more than 8,000 m (high mountains) have  
148 led to the development of a variety of floristic as well as vegetation patterns. Climate-dependent  
149 vegetation is largely determined by decreasing moisture and temperature with increasing  
150 elevations (thermal and hygrometric terrestrial lapse rates), which vary through time, affording  
151 opportunities for plant migrations, novel juxtapositions, and speciation. The Himalayan range to  
152 the north acts as a barrier to the southwest monsoon from the Bay of Bengal, causing the  
153 moisture regime to decrease westwards along the Siwaliks, and comparatively more rain is  
154 received in the East. The complex mountain topography creates diverse bioclimatic zones, an  
155 exceptionally rich biodiversity assemblage, and ‘sky’ island conditions for many species.  
156 Broadly, vegetation in the eastern Himalayas can be categorized into tropical, sub-tropical, warm  
157 temperate, cool temperate, sub-alpine, and alpine types in ascending order based on parameters

158 such as physiognomy, floral composition, habitat conditions, and physiography (WWF and  
159 ICIMOD 2001).

160 Takhtajan (1969) regarded the eastern Himalayas as the ‘cradle’ of flowering plants. The  
161 region is also well known for its botanically curious and rare species (e.g., *Sapria himalayana*  
162 Griff., Rafflesiaceae). Nearly 50% of the total flowering plants recorded in India are from the  
163 northeastern region. The genus *Rhododendron* (Ericaceae) is a remarkable taxon of showy  
164 plants, with most confined to this region and a substantial number of endemic species (Pradhan  
165 and Lachungpa, 1990). The eastern Himalayan region is rich in endemic floras and many species  
166 have value as medicinal or edible plants (Sundriyal, 1999).

167 Several species, namely *Shorea robusta* C.F. Gaertn., *Mesua ferrea* L., *Syzygium cumini*  
168 (L.) Skeels, *Terminalia paniculata* Roth., are dominant in northern tropical wet evergreen forests  
169 (150 m altitude); *Magnolia* L., *Terminalia elliptica* Willd., and *Bombax ceiba* L. in northern sub-  
170 tropical semi-evergreen forests (150–230 m); *Chukrasia tabularis* A. Juss., *Gmelina arborea*  
171 Roxb., *Rhododendron arboretum* Sm., *Dalbergia sissoo* Roxb. in North India moist deciduous  
172 forests (230–300 m); *Madhuca longifolia* (J. Konig) J.F. Macbr., *Gordonia chilaulia*,  
173 *Terminalia elliptica*, *Gossypium* L., *Toona ciliata* M. Roem. and *Cinnamomum glaucescens*  
174 (Nees) Hand. Mazz. in Northern sub-tropical broad-leaved wet forests (300–1,650 m altitude);  
175 *Senegalia catechu* (L. f.) P.J.H. Hurter & Mabb., *Abies densa* Griff., *Tsuga canadensis* Carrière,  
176 *Acer* L. in northern montane wet temperature forests (1,650–3,000 m); *Madhuca longifolia* (J.  
177 Konig) J.F. Macbr., *Schima wallichii* (DC.) Korth., *Castanopsis indica* (Roxb. ex Lindl.) A. DC.,  
178 *Terminalia elliptica*, *Duabanga grandiflora* Walp., *Cassia fistula* L., *Annona muricata* L. in east  
179 Himalayan moist temperature forests (1,500–1,800 m) and *Ficus religiosa* L., *Acer*,  
180 *Exbucklandia populnea* (R.Br. ex Griff.) R.W.Br., *Ceiba pentandra* (L.) Gaertn., *Prunus*

181 *undulata* Buch. Ham. ex D. Don, *Castanopsis* (D. Don) Spach, *Rhododendron* L., *Salix* L. in  
 182 sub-alpine forests (3,000–3,660 m) (Grierson and Long, 1983; Kaul and Haridasan, 1987; Hazra  
 183 et al., 1996; Baishya et al., 2001).

184 In and around the fossil localities the principal constituents of tropical moist semi-  
 185 evergreen to deciduous forests are *Pongamia pinnata* (L.) Pierre, *Bauhinia purpurea* L., *Albizia*  
 186 sp. L., *Dalbergia sisso* (Fabaceae); *Duabanga grandiflora* (D.C.) Walp., *Lagerstroemia*  
 187 *parviflora* Roxb. (Lythraceae); *Terminalia catappa* L., *T. chebula* Retz., *T. miocarpa* F. Muell.  
 188 (Combretaceae); *Litsea* sp. Lam., *Cinnamomum bejolghota* (Buch. Ham.) Sweet, *Actinodaphne*  
 189 *angustifolia* (Blume) Nees, *A. obovata* (Nees) Blume, *Phoebe goalparensis* Hutch. (Lauraceae);  
 190 *Gynocardia odorata* R.Br. (Achariaceae); *Calophyllum polyanthum* Wall. ex Choisy  
 191 (Calophyllaceae); *Bombax malabaricum* D.C. (Malvaceae); *Macaranga denticulata* (Blume)  
 192 Müll. Arg., *Mallotus* Lour. (Euphorbiaceae); *Knema* Lour. (Myristicaceae); *Elaeocarpus*  
 193 *aristatus* Roxb. (Elaeocarpaceae); *Shorea robusta* (Dipterocarpaceae); *Gmelina arborea* Roxb.  
 194 ex Sm., *Vitex quinata* (Lour.) F.N. Williams (Lamiaceae); *Dillenia pentagyna* Roxb.  
 195 (Dilleniaceae); *Sterculia villosa* Roxb. ex Sm., *Grewia eriocarpa* Juss., *Grewia zizyphifolia*  
 196 Baill. (Malvaceae); *Garuga pinnata* Roxb. (Bursereae); *Meliosma simplicifolia* (Roxb.) Walp.  
 197 (Sabiaceae); *Spondias axillaris* Roxb. B.L. Burtt & A.W. Hill (Anacardiaceae).

198

#### 199 **4. Research history of Palaeobotany in eastern Himalayan Siwalik**

200 The eastern Himalayas hosts many Cenozoic sedimentary basins that have yielded Siwalik  
 201 deposits that bear micro and mega plant fossils (Chakrobarty et al., 2020). The Lower, Middle,  
 202 and Upper Siwalik floral archives range from the middle Miocene to the early Pleistocene (Table  
 203 1). The first information about the occurrence of plant fossils in the eastern Himalaya Siwaliks

204 dates back to 1969 when Pathak (1969) initially described a few fragmentary angiosperm leaves  
205 from the middle Siwalik sediments of the Mahanadi section of Darjeeling. In subsequent years  
206 other geologists and paleobotanists also noted the presence of plant remains in the Siwalik  
207 sediments of the eastern Himalayas (Antal and Awasthi, 1993; Antal and Prasad, 1995, 1996a, b,  
208 c, 1997, 1998). During the last few decades plant fossil localities have increased and valuable  
209 contributions have been made to the knowledge of the Siwalik paleobotany of the eastern  
210 Himalayas (Mehrotra et al., 1999; Prasad and Tripathi, 2000; Joshi and Mehrotra, 2003a, b,  
211 2007; Mitra and Banerjee, 2004; Khan et al., 2007, 2008, 2009, 2011, 2014a, b, c, 2015a, b,  
212 2016, 2017a, b, 2018a, b, 2019a, b; Tripathi et al., 2007; Srivastava and Mehrotra, 2009; Khan  
213 and Bera, 2010, 2014a, b, 2016a, b, 2017; Prasad et al., 2015; Mehrotra et al., 2018; More et al.,  
214 2018; Srivastava et al., 2018). Rich and varied assemblages of plant megafossil, including leaf  
215 impressions, compressions, fruits, seeds, and woods, are now known and provide a sufficient  
216 basis for tracking regional environmental changes through time and space. Qualitatively, the  
217 present-day distribution of the taxonomically nearest living relatives (NLRs) of the Siwalik plant  
218 fossils suggests the existence of a tropical evergreen type of forest throughout the eastern  
219 Himalaya lowlands during the period of deposition. In recent years plant-based quantitative  
220 techniques (CLAMP - Climate Leaf Analysis Multivariate Program and CoA - Coexistence  
221 approach) have been used to derive past climate parameters (temperature, humidity, and  
222 precipitation) and chart monsoon evolution (Khan et al., 2014a, 2019b; Srivastava et al., 2021;  
223 Bhatia et al., 2022).

224

## 225 **5. Palaeofloristic composition**

226 This review is based on Siwalik (middle Miocene–early Pleistocene) plant megafossil  
227 assemblages recovered from the road and river exposures at different locations within the eastern  
228 Himalayas. The fossiliferous localities in the Darjeeling Siwalik sector are those of Oodlabari,  
229 Sevok road sections, and the Sevok bridge, Washbari, Gish, Lish, Churanthi, and Ramthi river  
230 sections; in Bhutan the Lakshmi and Darranga river sections and in the easternmost Siwalik  
231 sector, i.e., Southeastern Himalaya localities, the river cutting sections of the East Kameng  
232 district, the Bhalukpong, East Pinjoli and South Pinjoli road cutting sections of the West Kameng  
233 district, and the Naharlagun-Banderdewa, Nirjuli-Banderdewa, Itanagar-Banderdewa and  
234 Chandernagar-Gohpur road sections of the Papumpare district (Fig. 2). Most leaf impressions  
235 were preserved in grey shales. Here, we review 219 plant fossil taxa, of which 102 taxa are from  
236 Darjeeling foothills, 9 taxa are from Bhutan and 108 fossil taxa are from the Southeastern  
237 Himalaya. Most of the megafossil plant specimens were identified to the species level, but for a  
238 few specimens, necessary morphological characters were not preserved. Khan et al. (2015a,  
239 2016, 2017a, b) studied cuticular epidermal features of some compressed leaves from the  
240 Southeastern sub-Himalaya and those are the most securely identified specimens.

241 There have been several contributions describing plant macrofossils from the eastern  
242 Himalaya Siwaliks, but so far none has synthesized our knowledge of the past flora and  
243 environment throughout Siwalik sedimentation. The recovered megaplant remains include  
244 compressions and impressions of leaves, fruiting calyxes, fruits, seeds, petrified and carbonized  
245 woods (Figs. 3–5). The Siwalik floral assemblage is rich both in fossil quality and quantity and  
246 comprises 219 species belonging to 162 genera and 42 families (Tables 2 and S1–S5).  
247 Angiosperms are grouped into 159 genera within 39 families, the most abundant being the  
248 Fabaceae (represented by seventeen genera and twenty-four species), Dipterocarpaceae (four

249 genera and thirteen species), Annonaceae (eight genera and eleven species), Lauraceae (seven  
250 genera and eleven species), Euphorbiaceae (six genera and seven species), Anacardiaceae (six  
251 genera and six species), Flacourtiaceae (four genera and five species), Rubiaceae (four genera  
252 and five species), Apocynaceae (four genera and four species) and Meliaceae (three genera and  
253 four species) (Tables S4 and S5). The eastern Himalayan Siwalik fossil floras consist of a wide  
254 variety of mostly woody plants listed in Tables S1–S3. Arborescent taxa dominate the  
255 assemblage, grass, and ferns being in a minority. Additionally, some workers reported *in-situ*  
256 occurrences of characteristic epiphyllous fungi on Siwalik leaf megafossils (Table S6). Reliable  
257 identification of the fossils is crucial for reliable palaeoclimatic and palaeoecological  
258 interpretation, thus, here some fossil specimens of uncertain affinities have been excluded from  
259 the listed fossil floras. The fossil specimens are held in the repository of the Palaeobotany–  
260 Palynology Section, Department of Botany, University of Calcutta.

261

### 262 5.1. The Lower Siwalik flora (middle Miocene)

263 The Lower Siwalik assemblage recovered from sediments exposed near Gish, Ramthi,  
264 Oodlabari, Sevok of Darjeeling, East and West Kameng of Southeastern Himalaya comprises  
265 mainly angiosperm plant remains attributable to 91 species within 65 genera belonging to 32  
266 families (Table S1; Antal and Awasthi, 1993; Antal et al., 1996; Antal and Prasad, 1996a; Joshi  
267 and Mehrotra, 2007; Khan et al., 2008; Srivastava and Mehrotra, 2009; Khan and Bera, 2014a;  
268 Khan et al., 2015). In this assemblage, 90 leaf fossils, one dicot fossil wood, one  
269 Thelypteridaceae fern, and one gymnosperm taxon have been reported. Of these, 22 species are  
270 new to the Siwalik palaeoflora and 19 have been identified as new to the Neogene flora of India.  
271 For example, Khan and Bera (2017) described *Pinus* on the basis of seed remains from the Dafla

272 Formation exposed around the West Kameng district in the Southeastern Himalaya. This report  
273 provides the first-ever fossil record of *Pinus* winged seeds from India. It is obvious from the list  
274 of fossil taxa (Table S1) from the lower Siwalik eastern Himalaya assemblages that the family  
275 Fabaceae, represented by eight genera (*Entada* Adans., *Dalbergia* L. f., *Derris* Lour., *Millettia*  
276 *Wight & Arn.*, *Cynometra* L., *Bauhinia* Plum. ex L., *Albizia* Durazz., *Pongamia* Adans., *Acacia*  
277 *Mill.*, and *Mastertia* L.), is the most dominant, followed by Lauraceae comprising four genera,  
278 Flacourtiaceae comprising four genera, Dipterocarpaceae comprising two genera, Annonaceae  
279 comprising two genera, Euphorbiaceae comprising of two genera and Combretaceae comprising  
280 two. The dominance of Fabaceae and the presence of Dipterocarpaceae is very significant from  
281 both palaeoecological and phytogeographical contexts.

282

### 283 5.2. The Middle Siwalik flora (late Miocene to Pliocene)

284 The Middle Siwalik assemblages recovered from sediments exposed from the fossil localities of  
285 Bhutan, Darjeeling, and Southeastern Himalaya represent mainly angiosperm plant remains  
286 currently comprising 81 species of 56 genera within 29 families (Table S2). Assignments are  
287 based mainly on leaf impressions. In this assemblage, 67 leaf fossils, four dicot fossil wood  
288 specimens, and one Thelypteridaceae fern have been described. They show closed affinity with  
289 extant thermophilic taxa such as *Mitrephora* Hook. f. & Thomson, *Dipterocarpus* C.F. Gaertn.,  
290 *Combretum* Loef l., *Millettia*, *Donax* Lour. (*Clinogyne grandis* accepted name *Donax*  
291 *canniformis*), *Shorea*, *Meiogyne* Miq., *Fissistigma* Griff., *Gynocardia* R. Br., *Vatica* L., and  
292 *Garcinia* L. (Antal and Prasad, 1996a; Mehrotra et al., 1999; Prasad and Tripathi 2000; Tripathi  
293 et al., 2007; Prasad et al., 2015; Khan et al., 2016, 2017a, 2019). Of these, 17 species are new to  
294 the Siwalik flora and 15 have been identified as new to the Neogene flora of India.

295 Dipterocarpaceae, represented by 13 genera, is most dominant in the assemblage, followed by  
296 Annonaceae comprising four genera, Lauraceae comprising four genera, Sterculiaceae  
297 comprising two genera, and Calophyllaceae comprising two genera.

298

### 299 5.3. *The Upper Siwalik flora (late Pliocene to early Pleistocene)*

300 The upper part of the Siwalik assemblage recovered from sediments exposed near  
301 Papumpare, East and West Kameng of Southeastern Himalaya is mainly represented by dicots  
302 comprising 47 species of 31 genera belonging to 21 families (Table S3). Assignments are based  
303 on both leaf impressions and compressions. An exception is that part of a compressed tree fern  
304 axis with leaf and adventitious root scars in the unusual arrangement has been described from the  
305 Plio-Pleistocene sediments of Southeastern Himalaya (Bera et al., 2014). This was the first  
306 macroscopic record of a cyatheaceous fern from the Indian Cenozoic. Other specimens show  
307 affinity with extant angiosperm taxa such as *Dipterocarpus*, *Calophyllum* L., *Actinodaphne*  
308 Nees, *Shorea*, *Mastixia* Blume, *Gynocardia*, *Millettia*, *Knema* Lour., *Macaranga* Thouars,  
309 *Canarium* L., *Quercus* L., *Croton* L., *Gmelina* L., *Kayea* Wall., *Elaeocarpus* L., and *Pongamia*  
310 (Bera et al., 2004; Joshi and Mehrotra, 2007; Khan et al., 2011, 2015, 2016, 2017a, b; Khan and  
311 Bera, 2014a; Srivastava et al., 2018; Mehrotra et al., 2018). Lauraceae, represented by four  
312 genera, is the most dominant in this assemblage, followed by Fabaceae and Calophyllaceae  
313 represented by two genera.

314

### 315 **6. Floristic changes throughout the Siwalik succession**

316 The nearest living relatives (NLR) method extrapolates the known climatic requirements of  
317 modern taxa back to comparable and related taxa in the past and presupposes that fossil plants



318 and their modern relatives share similar physiological requirements for climate (Mosbrugger and  
319 Utescher, 1997). The megafossil assemblages recovered from the Siwalik sediments of the  
320 eastern Himalayas have yielded mainly angiosperm taxa (Tables S1–S3) that can be used  
321 effectively to interpret palaeoclimate and palaeoflora because the nearest living relatives of these  
322 fossil angiosperm taxa are known with high confidence. On the basis of NLRs, the Siwalik floral  
323 assemblages of the eastern Himalayas consist of three major forest elements: evergreen  
324 (58.60%), deciduous (26.82%), and others (14.39%) (Fig. 6a–d). In the eastern Himalayan  
325 Lower Siwalik assemblage 63.73% of the taxa are evergreen, and deciduous elements make up  
326 just 23.07% of the taxa (Fig. 6a). In the Middle Siwalik assemblage, 57.74% of the taxa are  
327 evergreen and 25.35% of taxa are deciduous (Fig. 6b). In the Upper Siwalik 54.34% and 32.60%  
328 are evergreen and deciduous respectively (Fig. 6c). With respect to the present-day distribution  
329 pattern of NLR taxa this suggests that wet evergreen forests persisted throughout the period of  
330 deposition (Tables S1–3; Fig. 6d). The predominance of evergreen elements in the assemblage  
331 along with pteridophytes (ferns) indicates the prevalence of a tropical, warm, humid climate with  
332 abundant rainfall in contrast to the relatively dry present-day climate in the area. An increase in  
333 deciduous elements is evident towards the close of the Middle Siwalik and the beginning of the  
334 Upper Siwalik (Fig. 6e). This change in the vegetation pattern must reflect a climatic change  
335 between the lower part (Miocene) and upper part of Siwalik (Plio-Pleistocene) deposition, and  
336 seems to indicate an increase in rainfall seasonality. We reconstruct the paleovegetation to better  
337 understand the general evolutionary history of floristic patterns in eastern Himalaya during  
338 Siwalik sedimentation (Fig. 7).

339

## 340 **7. Palaeoclimates reflected by the fossil floras**

341 Investigations using different qualitative (NLR, cuticular studies) and quantitative (Co-  
342 existence Approach and CLAMP) proxies have revealed the history of past climate, and in  
343 particular the evolution of Indian summer monsoon (ISM), during the Siwalik sediments of the  
344 eastern Himalayas (Khan and Bera, 2014a, b; Khan et al., 2014a, 2015, 2019a, b; Prasad et al.,  
345 2015; Srivastava et al., 2021; Bhatia et al., 2022).

346

### 347 *7.1. A qualitative NLR approach*

348 The principal basis of any study of the past is that known as 'uniformitarianism'. This,  
349 principle, often summarized as 'the present is the key to the past', implies that the physical and  
350 biological processes that operate in today's environment, as well as vegetation, must have  
351 functioned in a similar way in the past (Thanukos, 2012). In the case of the NLR approaches  
352 used to reconstruct past climates, this extrapolates the known climatic requirements of modern  
353 taxa to presumed ancestral taxa in the past. Of the plant fossils recovered from the eastern  
354 Himalayas that have nearest living relatives, several still exist in the area today. This suggests  
355 some degree of climatic similarity between the past and now and the persistence of a tropical  
356 warm and humid climate.

357

### 358 *7.2. The Coexistent Approach (CoA)*

359 CoA, developed by Mosbrugger and Utescher (1997), is based on the concept that the  
360 climatic requirements of fossil species are similar to those of their NLRs and reconstructs the  
361 paleoclimate parameters for a given fossil flora using climatic intervals in which all the NLRs of  
362 the fossil flora could coexist coexist (Mosbrugger and Utescher, 1997; Mosbrugger, 1999;  
363 Utescher et al., 2014). This is an improvement from many previous NLR analyses that have

364 tended to choose single, or at best, just a few taxa for the analysis. By adopting a whole-  
365 population approach, outliers due to misidentification or evolutionary innovation can be isolated  
366 and removed from the analysis, thus, improving accuracy and precision. Prasad et al. (2015) first  
367 reconstructed the eastern Siwalik palaeoclimate by applying this quantitative method to the  
368 middle Siwalik flora of Darjeeling sub-Himalaya. They estimated different climatic variables,  
369 such as mean annual temperature (MAT), warmest month mean temperature (WMMT), coldest  
370 month mean temperature (CMMT), and mean annual precipitation (MAP) as 22–26.5 °C, 17.8–  
371 20 °C, 25–30 °C, and 2650–3200 mm, respectively. However, their methodology differed from  
372 that codified by Mosbrugger and Utescher (1997) and Utescher et al. (2014) and did not specify  
373 the origins of their plant distribution data. Srivastava et al. (2021) subsequently reconstructed the  
374 climate of the Upper Siwalik strata of Southeastern Himalaya quantitatively, based on the more  
375 usual form of CoA specified by Mosbrugger and Utescher (1997) and Utescher et al. (2014), and  
376 reported that during the late Pliocene–early Pleistocene, the temperature seasonality between  
377 warm (27–28.1 °C) and cold months (22–23.6 °C) was less pronounced compared with present-  
378 day warm (27–27.7 °C) and cold (14.8–15.4 °C) month conditions. The reconstructed rainfall  
379 data indicated a monsoonal type of climate having a strong wet/dry seasonality during the  
380 deposition of the Upper Siwalik sediments. Recently, Bhatia et al. (2022) also applied this  
381 methodology to two Siwalik floras recovered from the Lower (middle Miocene) and Middle (late  
382 Miocene–Pliocene) Siwalik successions of Darjeeling in the eastern Himalayas. The  
383 reconstructed climate data suggested a decrease in both winter temperature and precipitation  
384 during the wettest months, and thus an overall drying, from the Lower to Middle part of the  
385 Siwalik succession.

386

387

388 *7.3. The CLAMP Approach*

389       The principal leaf-based palaeoclimate proxy for assessing a range of climate variables is  
390 known as CLAMP (Climate Leaf Analysis Multivariate Program; <http://clamp.ibcas.ac.cn>)  
391 (Wolfe, 1993; Kovach and Spicer, 1996; Yang et al., 2011, 2015). CLAMP utilizes the universal  
392 relationships that exist between leaf form in woody dicotyledonous plants and an array of climate  
393 variables. On a global scale, aggregate leaf form in a stand of vegetation is more strongly  
394 determined by climate than by taxonomic composition (Yang et al., 2015). Using a multivariate  
395 statistical engine, CLAMP decodes these relationships and, by scoring fossil leaf traits the same  
396 way as for living vegetation growing under known climatic regimes, estimates past conditions  
397 (<http://clamp.ibcas.ac.cn>). Five fossil floras (one lower Siwalik mid-Miocene, one middle  
398 Siwalik Pliocene, and one upper Siwalik Plio–Pleistocene flora of Southeastern Himalaya; one  
399 lower Siwalik mid-Miocene flora of Darjeeling and one latest Miocene-Pliocene middle Siwalik  
400 Group of Bhutan sub-Himalaya) ranging in age from the mid-Miocene to the early Pleistocene  
401 from the eastern Siwalik near Bhutan, Darjeeling and in Southeastern Himalaya were also  
402 subjected to a CLAMP analysis using a calibration data set that includes sites from India,  
403 southern China, and Thailand and gridded climate data (Khan et al., 2014a, 2019b) (Tables S7–  
404 S11). CLAMP climate retrodictions derived from the PhysgAsia2 calibration for all the fossil  
405 sites of the eastern Himalayas are given in Tables 3–5.

406       The results of these analyses are also consistent with published quantitative climate data  
407 (Khan et al., 2014a, 2019b) using CLAMP analysis (Wolfe, 1993; Teodoridis et al., 2011; Yang  
408 et al., 2011) on fossil leaf morphotypes (i.e., not assigned taxonomic affiliation) from the eastern  
409 Himalayas. Two lower Siwalik mid-Miocene floras of Darjeeling and Southeastern Himalaya

410 yielded almost the same values suggesting mean annual temperatures (MATs) of 25.4 and 25.3 ±  
411 2.8 °C (all uncertainties ±2 sigma) with warm month mean temperatures (WMMTs) of 28.4 and  
412 27.8 ± 3.39 °C and cold month mean temperatures (CMMTs) of 17.9 and 21.3 ± 4 °C.

413 Precipitation estimates have high uncertainties but suggest a weak monsoon with growing season  
414 precipitations of 181 ± 91 cm for Bhutan, 242 ± 92 cm for Darjeeling, and 174 ± 92 cm for AP.

415 Leaves from the middle Siwalik (Pliocene) sediments of Southeastern Himalaya indicate a  
416 lowering of the MAT to 23.7 °C, which appears to be largely a function of cooler winter months  
417 (CMMT 16.9 °C). Southeastern Himalaya's early Pleistocene temperatures and rainfall were  
418 similar to those of the mid-Miocene. Khan et al. (2019b) compared palaeoclimate estimates of  
419 the latest Miocene–Pliocene Siwalik (*ca.* 6 to 3.8 Ma) flora of Bhutan with those of Siwalik  
420 floras from the Miocene-Pleistocene of Southeastern Himalaya and the Miocene Siwalik flora of  
421 Darjeeling. Because all the Siwalik floras of the eastern Himalayas spanning the mid-Miocene to  
422 Pleistocene yield almost the same values, they suggested that overall, the eastern Himalayan  
423 Siwalik climate appears to have been remarkably uniform over the past 15 million years. The  
424 MAT result of the Bhutan Siwalik palaeoflora differs by just 0.6 °C from the Southeastern  
425 Himalaya, and 1.2 °C from the Darjeeling palaeoflora. For all Siwalik fossil assemblages,  
426 WMMTs, CMMTs, LGSs (length of the growing season), RH (mean annual relative humidity),  
427 and SH (mean annual specific humidity) are similar and consistent (WMMTs around 28 °C,  
428 CMMTs around 18 °C, LGSs around 12 months, RHs around 80% and SHs around 14 g/kg).

429 Hence, palaeoclimate estimates of the Southeastern Himalaya, Darjeeling, and Bhutan Siwalik  
430 flora provide valuable insights into monsoon climatic evolution throughout the eastern  
431 Himalayan Siwalik belt during late Cenozoic time and indicate that the Siwalik floras  
432 experienced a persistent monsoonal tropical warm humid climate. Changes in the Monsoon

433 index suggest that in both the Bhutan and Southeastern sub-Himalaya, there has been little  
434 change in the intensity of the monsoon since mid-Miocene time, while further west in the  
435 Darjeeling area precipitation seasonality has increased since the mid-Miocene.

436

### 437 *7.3.1. New insights into the thermal and hydrological regime of the eastern Himalayan Siwalik*

438 Here, we re-analyze the five well-documented fossil leaf assemblages from across the  
439 eastern Himalayas spanning Siwalik time (middle Miocene to early Pleistocene). All have been  
440 previously analyzed for the eleven standard CLAMP climate variables (mean annual temperature  
441 – MAT; warm month mean temperature – WMMT; cold month mean temperature – CMMT;  
442 length of the growing season – LGS; growing season precipitation – GSP; mean monthly  
443 growing season precipitation – MMGSP; precipitation during the three consecutive wettest  
444 months – 3WET; precipitation during the three consecutive driest months – 3DRY; mean annual  
445 relative humidity – RH. ANN; mean annual specific humidity – SH.ANN; and mean annual  
446 moist enthalpy – ENTH), calibrated using modern gridded climate data at 10' spatial resolution  
447 (HiResGridMetAsia2) and physiognomic PhysgAsia2 calibration (Table S12). Here, fossil leaf  
448 assemblages are subjected to a CLAMP analysis using a new high spatial resolution 30" (~1  
449 km<sup>2</sup>) WorldClim2 gridded climate data (Fick and Hijmans 2017; <http://worldclim.org/version2>)  
450 (Table S13) with 15 new climate variables (Tables 2–4; Figs. 8 and S1–S4). However, we use  
451 the same modern vegetation trait scores as used previously (PhysgAsia2) (Table S12). This  
452 calibration data set interpolates average meteorological observations between 1970 and 2000  
453 onto a spatial grid approximating 1 km<sup>2</sup>. CLAMP climate retrodictions for all the fossil sites of  
454 the eastern Himalayas are given in Tables 3–5.

455 One advantage of using WorldClim2 for calibration is that numerous environmental  
456 variables have been mapped onto the same grid, so for CLAMP, the range of environmental  
457 signals decoded from leaf form can be extended. The new temperature-related environmental  
458 variables that correlate strongly with leaf form are (1) the compensated thermicity index –  
459 THERM (sum of mean annual temperature, minimum temperature of the coldest month, the  
460 maximum temperature of the coldest month,  $\times 10$ , with compensations for better global  
461 comparability), (2) growing degree days above 0 °C – GDD\_0 (sum of mean monthly  
462 temperature for months with mean temperature  $> 0$  °C multiplied by the number of days this  
463 occurs), (3) growing degree days above 5 °C – GDD\_5 (Sum of mean monthly temperature for  
464 months with mean temperature  $> 5$  °C multiplied by the number of days this occurs), (4)  
465 minimum temperature of the warmest month – MIN\_T\_W (lowest daily temperature during the  
466 warmest month) and (5) maximum temperature of the coldest month – MAX\_T\_C (warmest  
467 daily temperature during the coldest month). The new humidity-related variables are (6) mean  
468 annual vapour pressure deficit – VPD.ANN, (7) mean summer vapour pressure deficit –  
469 VPD.SUM (average vapour pressure deficit during the three summer months), (8) mean winter  
470 vapour pressure deficit – VPD.WIN (average vapour pressure deficit during the three winter  
471 months), (9) mean spring vapour pressure deficit – VPD.SPR (average vapour pressure deficit  
472 during the three spring months), (10) mean autumn vapour pressure deficit – VPD.AUT (average  
473 vapour pressure deficit during the three autumn months), (11) mean annual potential  
474 evapotranspiration – PET.ANN (the ability of the atmosphere to remove water through  
475 evapotranspiration, given unlimited water supply-- no limits on plant water supply-- averaged  
476 over the year), (12) mean monthly potential evapotranspiration during the warmest quarter –

477 PET.WARM and (13) mean monthly potential evapotranspiration during the coldest quarter –  
478 PET. COLD.

479 Tables 3–5 present results obtained for the fossil assemblages using the new WorldClim2  
480 CLAMP calibration, as well as (for comparison) previously obtained results (in parentheses) that  
481 used low spatial resolution HiResGridMetAsia2CLAMP calibration. Figs. 8 and S1–S4 illustrate  
482 the CLAMP regression models for each of the climate variables to show not only the relative  
483 position on the regression of the Siwalik fossil locations but also the scatter of the modern  
484 training data and thus the precision of the CLAMP predictions. As used in earlier CLAMP  
485 analyses, all regression models are derived from the leaf physiognomy/climate relationships in  
486 four-dimensional space (Spicer and Herman, 2010). CLAMP scoresheets for all eastern  
487 Himalayan Siwalik fossil assemblages are given in the Tables S7–S11. The new WorldClim2-  
488 based climate training set (WorldClim2\_3br) and the accompanying modern leaf physiognomic  
489 (PhysgAsia2) data files are given in the Tables S12 and S13.

490 The new calibration and range of climate variables allow us to explore new insights into  
491 the hydrological regime. We examine not only precipitation but humidity in terms of specific  
492 humidity (SH), relative humidity (RH), vapour pressure deficit (VPD), and potential  
493 evapotranspiration (PET). Both VPD and PET are investigated in respect of annual average  
494 values and seasonal variations.

495 Using leaf form (physiognomy) we reconstruct middle Miocene–early Pleistocene thermal  
496 and hydrological regimes at five locations in the eastern Himalayas. The new high spatial  
497 resolution (~1 km) WorldClim2 calibration yields result similar to previous analyses, but also  
498 provides more detailed insights into the hydrological regime through the return of annual and  
499 seasonal vapour pressure deficit (VPD), potential evapotranspiration (PET) estimates, as well as



500 new thermal overviews through measures of thermicity and growing degree days. The new  
501 results confirm the overall warmth of the region. Palaeo-rainfall estimates have large  
502 uncertainties due to moisture not being limiting in the context of the Siwalik assemblages and  
503 because fossils are usually preserved in water-lain deposits, suggesting the parent plants were  
504 growing in or near year-round wet soils. The new measures of VPD and PET show the persistent  
505 high humidity to which the leaves were exposed and adapted, but with notably lower humidity  
506 during the summers at all the eastern Himalayan locations.

507

#### 508 7.4. Cuticular approach

509 No proxy is perfect, so a multiproxy approach is always desirable. The examination of fossil leaf  
510 cuticles found on compressed leaves can also afford an estimation of past climate. Several  
511 cuticular characters indicate a warm, humid tropical climate with non-limiting rainfall, including  
512 thin cuticles, undulate to sinuous epidermal lateral walls, non-papillate or smooth leaf external  
513 surfaces, few epidermal hairs, unspecialized stomata, and subsidiary cells, all of which are  
514 commonly found in the Siwalik assemblages (Khan et al., 2015a). The hypostomatic nature of  
515 many Siwalik stomata also reflects heavy precipitation, humidity, and shade. Cuticular micro-  
516 morphological features have also helped to confirm the identification of some leaf compressions  
517 to the species level, and are clearly indicative of mesophytic ecological conditions that reflect a  
518 tropical climate with high precipitation (Khan et al., 2015a, 2016, 2017a, b).

519 Some workers (Mitra and Banerjee, 2000; Mitra et al., 2002; Das et al., 2007; Mandal et  
520 al., 2009, 2011; Vishnu et al., 2017, 2019; Bera et al., 2018, 2019, 2022a, b; Khan et al., 2018b,  
521 2019c) reported *in-situ* occurrences on leaf megafossils of characteristic epiphyllous fungi such  
522 as *Meliolinites* (fossil Meliolaceae) (comparable to the modern genus *Meliola* Fr.), *Phomites*

523 (comparable to the modern genus *Phoma* Sacc.), *Palaeocercospora* (comparable to the modern  
524 genus *Cercospora* Fresen. ex Fuckel), *Palaeocolletotrichum* (comparable to the modern genus  
525 *Colletotrichum* Corda), *Palaeoasterina* (comparable to the modern genus *Asterina* Lév.) and  
526 *Vizellopsidites* (comparable to modern genus *Vizella* Sacc.) on the cuticular surfaces of fossilized  
527 leaf cuticle fragments of the different angiosperm taxa recovered from the Siwalik sediments  
528 (middle Miocene to early Pleistocene) of Darjeeling, Bhutan, and Southeastern Himalaya (Table  
529 S6). They described fossil fungi on the basis of vegetative and reproductive structures. The  
530 Siwalik host leaves harboring the fossil fungi so far identified are *Shorea*, *Dipterocarpus*  
531 (*Dipterocarpaceae*), *Breonia* A. Rich. ex D.C. (*Rubiaceae*), *Dysoxylum* Blume (*Meliaceae*),  
532 *Combretum* (*Combretaceae*), *Xylopia* L. (*Annonaceae*), *Amherstia* Wall. (*Fabaceae*),  
533 *Actinodaphne* Nees, *Lindera* Thunb, *Persea* (*Lauraceae*), *Macaranga* Thouars (*Euphorbiaceae*),  
534 *Lauraceae*, and *Poaceae*. Based on earlier records, it is also evident that *Lauraceae* has been a  
535 common host for meliolaceous fungi since the early Cenozoic (Khan et al., 2019c). The reported  
536 appreciable numbers of foliicolous fungal remains indicate the prevalence of a warm, humid,  
537 climate favored by the high rate of precipitation in the eastern Himalayas during the Plio-  
538 Pleistocene (Das et al., 2007; Bera et al., 2018, 2019, 2022a, b; Khan et al., 2018b; 2019c;  
539 Mandal et al., 2009, 2011; Mitra and Banerjee, 2000; Mitra et al., 2002; Vishnu et al., 2017,  
540 2019). These climatic data are also consistent with published climatic data obtained from the  
541 study of the macroscopic plant remains using qualitative and quantitative methods. Thus, for the  
542 eastern Himalayan Siwalik, all approaches (CLAMP, NLR, CoA, and cuticle) give broadly  
543 similar palaeoclimate outcomes. The *in-situ* evidence of epiphyllous fungal remains on host leaf  
544 cuticles also indicate the possible existence of a host-ectoparasite relationship in the ancient

545 warm and humid tropical evergreen forest of this area during Siwalik sedimentation (Vishnu et  
546 al., 2017, 2019; Bera et al., 2018, 2019, 2022a, b; Khan et al., 2018b, 2019c).

547

## 548 **8. Comparisons**

### 549 *8.1. Comparisons with other Siwalik floras*

550 To reveal the degree of resemblance to other Siwalik floras (western and central), we make  
551 the following comparisons.

552

#### 553 *8.1.1. Western Siwalik flora*

554 This includes the floras of Jammu and Kashmir, Uttarakhand, and Himachal Pradesh and  
555 comprises a large number of fossil woods and leaves (Sahni, 1964 a, b, Lakhanpal, 1965, 1967;  
556 Verma, 1968; Lakhanpal and Awasthi, 1992; Prasad, 1994, 2006; Prasad et al., 1997; Shashi et  
557 al., 2006, 2008; Srivastava et al., 2015). The NLRs of common fossil taxa are *Millettia*, *Ziziphus*  
558 *Mill*, *Pongamia*, *Dalbergia*, *Diospyros*, *Fissistigma*, *Bambusa* Schreb., *Dipterocarpus*,  
559 *Lagerstroemia*, *Marantochloa* Brongn. ex Gris, *Calophyllum*, *Shorea*, *Gynocardia*, *Grewia*,  
560 *Cynometra*, *Persea*, *Sterculia*, *Mallotus*, *Terminalia*, and *Hopea* Roxb. This indicates that these  
561 taxa were widely distributed in both eastern and western Siwalik strata and flourished under a  
562 generally equitable climate, at least in terms of temperature.

563

#### 564 *8.1.2. Central (Nepal) Siwalik flora*

565 Plant megafossils (mainly fossil leaves) are known from various localities in Nepal such as  
566 Koilabas, Arung Khola, Surai Khola, Tinau Khola, Babai and Surkhet Valleys, Mahendra  
567 Highway, Arjun Khola, and Sindhuli (Prakash and Prasad, 1984; Prasad, 1990, 1994b; Prasad et

568 al., 1997, 1999; Tripathi et al., 2002; Dwivedi et al., 2006; Prasad and Dwivedi, 2007).  
 569 Comparison of the eastern Himalaya fossil floras with those of the central Siwalik fossil flora  
 570 assemblages shows that most NLRs of the fossil genera *Mesua* L., *Mangifera* L., *Bouea* Meisn.,  
 571 *Garcinia*, *Albizia*, *Cassia* L., *Millettia*, *Ziziphus*, *Pongamia*, *Dalbergia*, *Diospyros*, *Fissistigma*,  
 572 *Bambusa*, *Dipterocarpus*, *Lagerstroemia*, *Marantochloa*, *Calophyllum*, *Shorea*, *Gynocardia*,  
 573 *Grewia*, *Cynometra*, *Persea*, *Sterculia*, *Melilotus*, *Cinnamomum* Schaeff., *Mitrephora* Hook. f. &  
 574 Thomson, *Hopea*, *Polyalthia* Blume, *Uvaria* L., *Sabia* Colebr., *Miliusa* Lesch. ex A. D.C.,  
 575 *Swintonia* Griff., *Euphorbia* L., *Entada*, *Combretum*, *Dillenia*, *Randia* L., and *Flacourtia* Comm.  
 576 ex L. 'Hér. are common to both regions.

577

## 578 8.2. Comparisons among Siwalik CLAMP data

### 579 8.2.1. Methodology

580 The CLAMP methodology, its limitations, and its evolution are detailed in Spicer et al.,  
 581 (2021), but in summary, CLAMP reconstructs past climate based on an array of macroscopic leaf  
 582 traits preserved in leaf megafossils. Organic remains are not required and CLAMP can be  
 583 applied to mere leaf impressions provided that the leaves retain sufficient trait data across a  
 584 minimum of 20 taxa or morphotypes in any one fossil assemblage. Also, leaf identification is not  
 585 required, only an ability to distinguish one taxon (morphotype) from another. Morphotype  
 586 partitioning is based not only on the CLAMP traits (31 trait states encompassing leaf lobing,  
 587 margin features size, apex, base forms, and overall shape, but also venation and other  
 588 taxonomically useful features.

589 To calibrate CLAMP, a database of trait spectra from modern vegetation stands growing  
 590 under a wide range of known climate conditions provides a multidimensional framework for

591 identifying correlations between leaf trait combinations and individual climate variables such as  
592 temperature and moisture metrics. This physiognomic data set is accompanied by a suite of  
593 climate data derived in most cases from gridded observations. There are several such modern  
594 gridded data sets available at different spatial resolutions (e.g., New et al., 1999, 2002; Harris et  
595 al., 2014; Fick and Hijmans, 2017) and each are slightly different, largely as a function of  
596 interpolation artifacts and different observation periods, and so return slightly different  
597 retrodictions of past climate. This is shown in Tables 3 and 4 where WorldClim2 calibration  
598 results are compared with those based on New et al. (2002), shown in parentheses. These climate  
599 calibration anomalies apply to any climate proxy, so it is important when comparing proxy-  
600 reconstructed past climates that uncertainties introduced by using different types of climate  
601 calibration data are fully appreciated. Here we use a common proxy CLAMP calibration  
602 combining the PhysgAsia2 leaf trait data set (Spicer et al., 2020) with the WorldClim2 climate  
603 data gridded at  $\sim 1$  km resolution (Fick and Hijmans, 2017). The trait/climate relationships are  
604 decoded using the multivariate statistical engine known as Canonical Correspondence Analysis  
605 (ter Braak, 1996; <http://clamp.ibcas.ac.cn>).

606         Recently, fossil leaf assemblages from the lower (middle Miocene) and middle (late  
607 Miocene-Pliocene) Siwalik sediments exposed in Nepal were subjected to a CLAMP analysis by  
608 Bhatia et al. (2021) using the new high spatial resolution ( $\sim 1$  km<sup>2</sup>) WorldClim2 gridded climate  
609 data and PhysgAsia2 calibration. Their analysis indicates a mean annual temperature (MAT) of  
610  $22.2 \pm 2.3$  °C and  $24.7 \pm 2.3$  °C for the Lower Siwalik and Middle Siwalik assemblages,  
611 respectively. Cold month mean temperatures (CMMTs) were  $14.7$  and  $19 \pm 3.5$  °C and warm  
612 month mean temperatures (WMMTs) were  $28.3$  and  $28.5 \pm 3$  °C for the Lower and Middle  
613 Siwalik assemblages, respectively, showing warming of the cold months being mostly

614 responsible for a slight increase in the MAT over that time interval. Here, we compare  
615 palaeoclimate estimates of the middle Miocene to Plio-Pleistocene Siwalik flora from the eastern  
616 Himalayas with those of previously investigated Siwalik middle Miocene-Pliocene floras of  
617 Nepal.

618 Tables 3-5 summarize the CLAMP results for the eastern Himalaya Siwaliks. Table 3  
619 focuses on temperature-related metrics while Table 4 provides an overview of rainfall-related  
620 metrics and Table 5 presents humidity-related metrics. All middle Miocene (Lower Siwalik of  
621 Southeastern Himalaya and Darjeeling) thermal metrics are identical within 1 sigma uncertainty,  
622 showing frost-free year-round growth in a climate where the CMMT is  $>18^{\circ}\text{C}$  and thus 'tropical'.  
623 The CMMT of the Lower Siwalik of Nepal is somewhat lower at  $14^{\circ}\text{C}$  and just on the margins  
624 of the 1 sigma uncertainty difference from the eastern Himalaya value reported here. This  
625 marginal difference is also evident in the cooler ( $21^{\circ}\text{C}$  for Nepal versus  $24.3$  and  $26.4^{\circ}\text{C}$  for  
626 Darjeeling and Southeastern Himalaya, respectively) maximum temperature of the coldest month  
627 metric, but again it is debatable whether these differences can be regarded as real. For the Middle  
628 Siwalik assemblages (late Miocene to Pliocene of Southeastern Himalaya and Bhutan) a similar  
629 pattern is evident with all thermal metrics showing no discernible differences between  
630 assemblages (Table 5). These values are also more or less identical to those from the Middle  
631 Siwalik of Nepal reported by Bhatia et al. (2021). There is only one Upper Siwalik (late Pliocene  
632 to Pleistocene) assemblage reported here from the eastern Himalayas and that is from the  
633 Southeastern Himalaya section. This also shows thermal metrics apparently unchanged from  
634 those of earlier times.

635 Regarding rainfall-related metrics (Table 4), the Lower Siwalik assemblages of Darjeeling  
636 and Southeastern Himalaya are identical within uncertainty except for precipitation during the

637 three consecutive driest months, which indicates Darjeeling was markedly wetter than  
638 Southeastern Himalaya. This difference is independent of which meteorological data set is used  
639 for calibration. The Middle Siwalik sites similarly are indistinguishable from one another, this  
640 time across all moisture metrics. The Darjeeling Lower Siwalik assemblage appears to be  
641 notably wetter than the other sites, particularly in respect of precipitation during the three  
642 consecutive driest months, but apart from that, all assemblages appear very similar in terms of  
643 their reconstructed climate metrics.

644         It is often assumed that rainfall is an important environmental constraint on plant growth,  
645 but this need not be the case. What is critical is soil moisture combined with transpirational  
646 stresses imposed by atmospheric humidity and wind strength. In situations where leaf fossils are  
647 preserved (i.e., near water bodies), soil moisture reflects the proximity to that water body, not  
648 necessarily local rainfall, and because of this, the soil moisture in these situations is rarely  
649 limiting. It follows that a more useful measure of atmospheric conditions can be found in the  
650 way that leaf traits code for humidity metrics, especially vapour pressure deficit (VPD) and  
651 potential evapotranspiration (PET) (Spicer et al., 2019, 2020). VPD is a measure of the ease by  
652 which a plant can lose moisture to the atmosphere, with low VPDs found when the air is near  
653 saturation and there is strong resistance to transpiration, whereas at high VPDs there is no  
654 atmospheric constraint on transpirational water loss from the plant. Unlike relative humidity  
655 (RH), VPD has a nearly straight-line relationship to the rate of evapotranspiration, and plant  
656 distribution (Huffaker, 1942) and leaf physiognomy (Spicer et al., 2019) are more reflective of  
657 VPD than RH. PET is similar but is a measure of the ability of the atmosphere to remove water  
658 through evapotranspirational processes provided the water supply to the roots is not limiting.  
659 Unlike with VPD, atmospheric dynamics (convection and wind) play a role in determining PET.

660 Table 5 suggests very similar values of humidity metrics among the different assemblages  
661 through time. That is to say, there are no discernable step changes in climate features from the  
662 mid-Miocene to the Pleistocene. However, there are some important seasonal differences in VPD  
663 and PET metrics consistent across all assemblages, with summer being consistently more humid  
664 than spring, as with the modern SAM, but Darjeeling shows less seasonal variation in VPD than  
665 at Bhutan or Southeastern Himalaya. This reflects the relatively wet dry season in Darjeeling as  
666 indicated by rainfall metrics (Table 4). Similarly, the cold month (winter) PET value is more  
667 than 1 standard deviation lower than the other cold month PET values, suggesting a markedly  
668 wetter dry season.

669 Because all the Siwalik floras of the eastern Himalayas and Central Himalayas yield almost  
670 the same values, we suggest that overall, the eastern and central Himalayan Siwalik climate  
671 appears to have remained remarkably uniform from the mid-Miocene to Pleistocene. However,  
672 while the modern temperature regime for the eastern Himalayan Siwaliks exhibits cooler winters  
673 than evident from the fossil data, the overall temperature regime is similar over time. The most  
674 marked differences are in the precipitation regime, with the modern being wetter with a greater  
675 seasonality in rainfall (wetter wet seasons and drier dry seasons) (Table S14). However, because  
676 uncertainties are also quite large for these metrics, the differences between the past and present  
677 may not be genuinely significant. It is unlikely that this consistency over time is representative  
678 of the whole SAM region, but it does have important implications for ecosystem evolution in the  
679 eastern Himalayas at low elevations, as discussed below.

680

## 681 **9. Plant-arthropod associations from Siwalik forests**



682 Fossil leaf impressions and compressions from the Siwalik sedimentary strata of the  
683 eastern Himalayas provide evidence of a variety of plant-insect interactions that have operated  
684 throughout the evolution of monsoon-influenced forests since middle Miocene times (Khan et  
685 al., 2014b, 2015b). Five functional feeding groups (FFGs) were identified in this study, namely  
686 leaf mining, hole feeding, skeletonizing, galling, and margin feeding. Furthermore, these  
687 morphotracers are similar to those found in leaves of extant plant species such as *Millettia*,  
688 *Canarium* L., *Glochidion* J.R. Forst. & G. Forst., *Callicarpa* L., *Chonemorpha* G. Don,  
689 *Actinodaphne*, *Persea*, *Woodfordia* Salisb., *Shorea*, *Artocarpus* J.R. Forst. & G. Forst., *Albizia*,  
690 *Lagerstroemia* and others, suggesting similar interactions have existed in the eastern Himalaya  
691 region for at least 15 million years. On the basis of comparison with extant taxa, possible leaf  
692 feeders could have belonged to the insect orders Orthoptera, Coleoptera, Lepidoptera, and  
693 Diptera, and those plant-arthropod relationships were established by the mid-Miocene and  
694 continue to the present, shaping both the present-day flora and fauna. Khan et al. (2014b, 2015b)  
695 also compared insect herbivory evident in the Darjeeling Lower Siwalik flora to that of the  
696 similarly aged Southeastern Lower Siwalik flora, as well as two younger floras from that area  
697 and noted a similar range of FFGs and damage types among all four fossil floras of the eastern  
698 Himalayas. They concluded that compared to biotic factors climate had little influence on  
699 determining the evolution of plant-insect interactions in the eastern Himalayan region.

700

## 701 **10. Phytogeographic patterns**

702 The Siwalik plant fossils date from the late Neogene time (middle Miocene to early  
703 Pleistocene), and close relatives of the fossil forms still exist in the tropical forests of India and  
704 Southeast Asia today. This allows direct tracking of changes in phytogeographic distributions of

705 these taxa over time. The present-day distributions of NLRs of 219 fossil taxa recovered from the  
 706 Siwalik sediments (Mio-Pleistocene) of the eastern Himalayas indicate that today they grow in a  
 707 variety of locations all over India and other adjoining countries (Fig. 9). In India, they are  
 708 distributed in the northeastern (14.75%) and southern regions (4.35%). In this Siwalik  
 709 assemblage, the NLRs of 49.04% taxa (*Shorea roxburghii* G. Don, *Uvaria hirsuta* A. St. Hil.,  
 710 *Dipterocarpus tuberculatus* Roxb., *D. turbinatus* Roxb., *Ventilago calyculata* Tul., *Syzygium*  
 711 *cuminii* (Gamble) Tenjarla & Kashyapa, *Homonoia riparia* Lour., *Xanthophyllum flavescens*  
 712 Roxb., *Mitrephora maingayi* Hook. f. & Thomson, *Hopea wightiana* Roxb., *Bauhinia accrescens*  
 713 Killip & J.F. Macbr., *Randia wallichii* Hook. f., *R. densiflora* Lou., *Fissistigma bicolor* Merr.,  
 714 *Bombax malabaricum* D.C., *Sterculia parviflora* Roxb., *Buchanania sessilifolia* Blume,  
 715 *Cynometra iripa* Kostel., *Calophyllum polyanthum* Wall. ex Choisy, *Glochidion zeylanicum*  
 716 (Gaertn.) A. Juss., *Pongamia pinnata* (L.) Merr. occur both in India and the Malaya Peninsula  
 717 and 22.7% taxa (*Pterospermum yunnanense* H.H. Hsue, *Parashorea buchananii* (C.E.C. Fisch.)  
 718 Symington, *Flacourtia inermis* Wall., *Fordia albiflora* (Prain) Dasuki & Schot, *Paranephelium*  
 719 *macrophyllum* King, *Diospyros argentea* Griff.) are found to generally grow in Malaya. This  
 720 clearly indicates a free exchange of floral elements during the late Neogene across Southeastern  
 721 Asia (Fig. 10).

722 The late Neogene floral assemblages covering the eastern Himalayas and Southeast Asian  
 723 countries (Sumatra, Borneo, Indonesia, Vietnam, Malaysia, and Java) not only reflect great  
 724 diversity with respect to the angiosperm families and variety of taxa but also uniformity and  
 725 similarity in floristic composition. Thus, the late Neogene may be regarded as the time of  
 726 maximum proliferation and diversification of tropical vegetation, particularly in the evergreen  
 727 forests in Southeast Asia (Bande and Prakash, 1986; Awasthi and Mehrotra, 1990, 1997; Guleria,

1992). This floral spread was not unidirectional but suggests cross-migration between the regions as some Southeast Asian taxa must have migrated from the Indian landmass due to the widespread distribution of similar edaphic and climatic factors. Evidence of many southeast Asian elements recovered from the Siwalik exposures of the eastern Himalayas suggest migration into the Indian subcontinent and intermixing and merging with the existing eastern Himalayan flora before expanding further westwards along the entire Himalayan lowlands. Hence, the late Neogene period may be considered an important time in the evolution and speciation of flowering plants in India and Southeast Asia through the introduction and proliferation of new floral elements and the opportunity for subsequent interbreeding.

#### **11. Disappearance of some plant taxa**

Gradual changes in climate and monsoon amplification across Asia during the Neogene (Su et al., 2013; Tang et al., 2013, 2015) have been attributed to a general global cooling (Zachos et al., 2001, 2008), closure of the Tethys, loss of littoral environments along the Himalayan front (Lakhanpal, 1970) and rapid uplift of the Himalayas (Chatterjee and Scotese, 1999; Ding et al., 2017; Molnar et al., 2010; Boos and Kuang, 2010; Farnsworth et al., 2019). These factors are all likely to have played an important role in altering and diversifying floral patterns (Huggett, 2004; Morley, 2000; Mosbrugger et al., 2005). Some plant taxa were able to adapt to the changed circumstances or already had wide environmental tolerances. These have continued to flourish to the present-day in the areas surrounding the fossil localities, whereas others that could not adapt to the new environment either suffered local extinction or shifted to suitable areas with more favourable eco-climatic conditions.

750 Based on the present-day distribution of NLRs of the eastern Himalayan Siwalik plant  
751 fossil species, we categorize the Siwalik species into three main groups: extant local species  
752 (65%), extant but locally extinct species (12%), and extant but regionally extinct species (23%)  
753 (Fig. 9b). Extant local species have their NLRs (for example, *Guatteria australis* A. St. Hil.,  
754 *Dipterocarpus tuberculatus* Roxb., *D. turbinatus* C.F. Gaertn., *Syzygium cuminii* (Gamble)  
755 Tenjarla & Kashyapa, *Tarennoidea wallichii* (Hook. f.) Tirveng. & Sastre, *Fissistigma bicolor*  
756 Merr., *Bombax ceiba* L., *Sterculia parviflora* Roxb., *Cynometra iripa* Kostel., *Calophyllum*  
757 *polyanthum* Wall. ex Choisy, *Glochidion zeylanicum* (Gaertn.) A. Juss., *Pongamia pinnata* (L.)  
758 Merr.) growing today in or near the fossil localities. Extant but locally extinct species (for  
759 example, *Mastixia arborea* (Wight) C.B. Clarke, *Shorea tumbuggaia* Roxb., *Persea parviflora*  
760 (Meisn.) Harid. & R.R. Rao, *Callerya cinerea* (Benth.) Schot, *Phyllanthus daltonii* Müll. Arg.,  
761 *Calophyllum inophyllum* L., *Lindera bifaria* Hosseus, *Premna bengalensis* C.B. Clarke etc.)  
762 grow in other parts of India, but do not occur in the present-day near the fossil localities.  
763 However, extant but regionally extinct NLRs (*Millettia extensa* (Benth.) Benth. ex Baker,  
764 *Dysoxylum costulatum* Blume, *Rourea caudata* Planch., *Sloanea dasycarpa* Hemsl., *Shorea*  
765 *leprosula* Miq., *S. obtusa* Wall. ex Blume etc.) have disappeared from India and now grow in  
766 other parts of the world. Given the apparent constancy of the climate in this region, we presume  
767 that significant changes in biotic interactions might be a reason for the disappearance of taxa  
768 from the present-day vegetation, including human activity. However, these taxa are presently  
769 growing in other regions of India, including the northeast region and south India, due to the  
770 availability of suitable conditions. If climate changes are involved, then they are subtler than can  
771 be detected by the CLAMP proxy given the existing statistical uncertainties.

772 The upper Paleocene record of *Calophyllum* in India (Bhattacharyya, 1967; Ambwani,  
773 1992) suggests India is the centre of origin of this genus. Subsequently, this genus gradually  
774 became a ubiquitous component of the Neogene Siwalik forests of India and moved into other  
775 adjoining Southeast Asian regions, Polynesia, and the east coast of Africa as evidenced by later  
776 records outside India (Khan et al., 2017a). Khan et al. (2017a) suggested that distinct, but  
777 modest, elevation changes in northeastern India, possibly related to Himalayan orogeny since the  
778 Miocene, might have caused the disappearance of *Calophyllum inophyllum* from the entire  
779 eastern Himalayas.

780 Based on fossil records Khan et al. (2016) suggested that *Shorea* was a common forest  
781 element in the Neogene (Miocene time) Siwalik forests of the eastern Himalayas. They also  
782 reviewed the historical phytogeography and highlighted the phytogeographic implications of this  
783 genus.

784 Several other low-elevation eastern Himalaya taxa have undergone range shifts since  
785 the mid-Miocene. According to Khan and Bera (2007), *Dysoxylum costulatum* probably migrated  
786 to the Malaya region after the Miocene. Khan and Bera (2017) suggested that *Pinus* was an  
787 important component of tropical-subtropical evergreen forest in the West Kameng district of  
788 Southeastern Himalaya during the Miocene but this conifer taxon subsequently declined from the  
789 local vegetation. At present, *Rourea caudata* (Connaraceae) does not grow in India and is  
790 confined to the tropical evergreen forest of southeast Asian regions (China and Myanmar) where  
791 conditions are more suitable. Khan and Bera (2016) suggested that this species of Connaraceae  
792 probably migrated to these Southeast Asian regions after lower Siwalik sedimentation (middle-  
793 upper Miocene).

794 Khan et al. (2017b) reported the occurrence of the extant species *Mastixia arborea* (family  
795 Cornaceae) from the middle Miocene to early Pleistocene Siwalik sediments of Southeastern  
796 Himalaya. This report provided the first-ever fossil record of Mastixioids from India, as well as  
797 Asia. At present, *M. arborea* does not grow in the eastern Himalayas but is endemic to the  
798 tropical evergreen forests of the Western Ghats. They suggested that its extinction from the  
799 entire eastern Himalaya and probable movement to the Western Ghats is likely due to climate  
800 change (Siwalik forests experienced a weaker monsoon, i.e., less rainfall seasonality than now)  
801 in the area, related to the Himalayan Orogeny during Miocene-Pleistocene times. They also  
802 suggested that its disappearance from present-day vegetation proximal to the fossil locality may  
803 be related to the gradual intensification of rainfall seasonality since the late Miocene. Such  
804 intensification is not evident in the CLAMP data. Similarly, More et al. (2018) reported *Sloanea*  
805 *dasycarpa* of Elaeocarpaceae from the Geabdat Sandstone Formation, Pliocene of Darjeeling  
806 foothills. They suggested that after the Pliocene the species might have migrated from the  
807 Darjeeling Himalayan region to adjoining southeast Asia (China, Myanmar, and Vietnam), the  
808 area of the present-day distribution of modern *Sloanea*, due to possible increasing aridity and  
809 rainfall seasonality, but again this is not evident in the data presented here.

810

## 811 **12. Conclusion**

812 This is the first thorough review of the eastern Himalayan Siwalik flora. Based on our  
813 overview of published palaeobotanical data from the Siwalik sediments, the following key points  
814 emerge:

815 (1) The eastern Himalaya has a rich Siwalik plant fossil record spanning the mid-Miocene to  
816 the Pleistocene, which, over the past two decades, has been investigated extensively with

817 an increasing number of fossil taxa being reported. These fossil taxa are important for  
818 answering outstanding questions on plant diversity and floral evolution in this region.

819 (2) Plant species from the Cenozoic of the eastern Himalayas are diverse. To date,  
820 approximately 219 fossil species belonging to 162 genera of 42 families have been  
821 documented. They cover ferns, gymnosperms, and angiosperms, of which angiosperms  
822 are by far the most diverse, including 216 fossil species grouped into 159 genera of 39  
823 families. In the fossil angiosperms, Fabaceae, Dipterocarpaceae, Lauraceae, Annonaceae,  
824 Euphorbiaceae, Calophyllaceae, Anacardiaceae, Apocynaceae, Rubiaceae, and  
825 Lythraceae are among the most diverse families; and *Shorea*, *Dipterocarpus*,  
826 *Calophyllum*, *Millettia*, *Glochidion*, *Actinodaphne*, *Combretum*, *Bauhinia*,  
827 *Lagerstroemia*, *Uvaria*, *Rinorea* Aubl., *Sterculia*, *Ficus* L., *Terminalia*, and *Persea* are  
828 among the most species-rich genera.

829 (3) Most of the families and genera represented in the fossil record are still part of the  
830 modern natural vegetation in the eastern Himalayas, but some taxa have disappeared.  
831 Thus far, fourteen taxa are known to have become extinct in the eastern Himalayas,  
832 namely *Mastixia arborea*, *Shorea tumbuggaia*, *S. leprosula*, *S. obtusa*, *Persea parviflora*,  
833 *Callerya cinerea*, *Phyllanthus daltonii*, *Calophyllum inophyllum*, *Lindera bifaria*,  
834 *Premna bengalensis*, *Millettia extensa*, *Dysoxylum costulatum*, *Rourea caudata*, and  
835 *Sloanea dasycarpa*. In addition, phytogeographic exchanges of Siwalik elements of the  
836 eastern Himalayas with southeast Asia also occur.

837 (4) A gradual change in floral composition through the Siwalik succession is apparent. Floras  
838 changed significantly from the middle Miocene to the early Pleistocene through to today,  
839 but invoking climate change as the explanation is problematic as no distinctive

840 (statistically significant) shift in climate metrics can be detected in foliar adaptations. If  
841 the climate contributed to these changes, it was through very subtle changes that affected  
842 overall taxon fitness, most likely intensification of rainfall seasonality.

843 (5) Here, we introduce new quantitative proxy palaeo-humidity measurements and explore  
844 new insights into the hydrological regime. Eastern Himalayan Siwalik forests  
845 experienced a monsoonal tropical warm humid climate. Tropical Siwalik forests of the  
846 eastern Himalaya prior to the Quaternary have a weaker monsoon (less rainfall  
847 seasonality) than now.

848

849

#### 850 **Acknowledgments**

851 MK and SM gratefully acknowledge the Department of Botany, Sidho-Kanho-Birsha University  
852 for providing infrastructural facilities to accomplish this work. SB acknowledges the Centre of  
853 Advanced Study (Phase-VII), the Department of Botany, the University of Calcutta for providing  
854 necessary facilities. We also thank Prof. Paul Valdes, Bristol University, U.K., for providing the  
855 modern WorldClim2 climate data for the fossil localities. RAS and TEVS were supported by  
856 NERC/NSFC BETR Project NE/P013805/1.

857

#### 858 **Disclosure statement**

859 No potential conflict of interest was reported by the authors.

860

#### 861 **Appendix A. Supplementary data**

862 Supplementary data to this article can be found online at:



863 **References**

- 864 Acharya, S.K., 1994. The Cenozoic foreland basin and tectonics of the eastern Sub-Himalaya:  
865 problem and prospects. *Himal. Geol.* 15, 3–21.
- 866 Acharyya, S.K., Bhatt, D.K., Sen, M.K., 1987. Earliest Miocene Planktonic foraminifera from  
867 Kalijhora area, Tista River section, Darjeeling sub-Himalaya. *Indian Min.* 41, 31–37.
- 868 Ambwani, K., 1992. Leaf impressions belonging to the Tertiary age of northeast India.  
869 *Phytomorphology* 41, 139–146.
- 870 Anand-Prakash, Singh, T., 2000. Nature, composition, rank (maturation) and depositional  
871 environment of Siwalik coals from Arunachal Himalaya. *Mycol. Prog.* 21, 17–29.
- 872 Antal, J.S., Awasthi, N., 1993. Fossil flora from the Himalayan foot-hills of Darjeeling district,  
873 West Bengal and its palaeoecological and phytogeographical significance. *Palaeobotanist*  
874 42, 14–60.
- 875 Antal, J.S., Prasad, M., 1995. Fossil leaf of *Clinogyne* Salisb. from the Siwalik sediments of  
876 Darjeeling district, West Bengal. *Geophytology* 24, 2412–43.
- 877 Antal, J.S., Prasad, M., 1996a. Some more leaf-impressions from the Himalayan foothills of  
878 Darjeeling district, West Bengal, India. *Palaeobotanist* 43, 1–9.
- 879 Antal, J.S., Prasad, M., 1996b. Dipterocarpaceous fossil leaves from Grish River section in  
880 Himalayan foot hills near Oodlabari, Darjeeling district, West Bengal. *Palaeobotanist* 43,  
881 73–77.
- 882 Antal, J.S., Prasad, M., 1996c. Leaf-impressions of *Polyalthia* Bl. in the Siwalik sediments of  
883 Darjeeling district, West Bengal. *Geophytology* 26, 125–127.
- 884 Antal, J.S., Prasad, M., 1997. Angiospermous fossil leaves from the Siwalik sediments (Middle-  
885 Miocene) of Darjeeling district, West Bengal. *Palaeobotanist* 46, 95–104.

- 886 Antal, J.S., Prasad, M., 1998. Morphotaxonomic study of some more fossil leaves from the lower  
887 Siwalik sediments of West Bengal, India. *Palaeobotanist* 47, 86–98.
- 888 Awasthi, N., Mehrotra, R.C., 1990. Some fossil woods from Tipam sandstone of Assam and  
889 Nagaland. *Palaeobotanist* 38, 277–234.
- 890 Awasthi, N., Mehrotra, R.C., 1997. Some fossil dicotyledonous woods from the Neogene of  
891 Arunachal Pradesh, India. *Palaeontogra. Abt. B* 245, 109–121.
- 892 Baishya, A.K., Haque, S., Bora, P.J., et al., 2001. Flora of Arunachal Pradesh — an overview.  
893 *Arunachal Floral News* 19, 1–24.
- 894 Bande, M., Prakash, U., 1986. The Tertiary flora of Southeast Asia with remarks on its  
895 palaeoenvironment and phytogeography of the Indo-Malayan region. *Rev. Paleobot.*  
896 *Palynol.* 49, 203–233.
- 897 Bera, S., A. De., B. De. 2004. First record of *Elaeocarpus* Linn. fruits from the upper siwalik  
898 sediments (Kimin formation) of Arunachal Pradesh, India. *J. Geol. Soc. India.* 64, 350–  
899 352.
- 900 Bera, M., Khan, M.A., Bera, S., 2018. Two new species of *Phomites* Fritel from the phyllosphere  
901 of Siwalik. *J. Mycopathol. Res.* 56, 11–14.
- 902 Bera, M., Khan, M.A., Bera, S., 2019. A new foliicolous melioloid fungus from the Pliocene of  
903 eastern Himalaya. *Mycol. Prog.* 18, 921–931.
- 904 Bera, M., Khan, M.A., Acharya, K., et al., 2022a. In situ occurrence of *Phomites* Fritel in the  
905 Phyllosphere of ancient Siwalik forests of eastern Himalaya during the Mio-Pleistocene.  
906 In: M. Rai et al. (eds.). *Phoma: Diversity, Taxonomy, Bioactivities, and Nanotechnology*,  
907 [https://doi.org/10.1007/978-3-030-81218-8\\_18](https://doi.org/10.1007/978-3-030-81218-8_18)

- 908 Bera, M., Khan, M.A., Hazra, T., et al., 2022b. A novel fossil-species of *Meliolinites* Selkirk  
909 (fossil Meliolaceae) and its life cycle stages associated with an angiosperm fossil leaf from  
910 the Siwalik (Mio-Pliocene) of Bhutan sub-Himalaya. *Fungal Biol.* 126, 576–586.
- 911 Bera, S., Gupta, S., Khan, M.A., et al., 2014. First megafossil evidence of Cyatheaceous tree fern  
912 from the Indian Cenozoic. *J. Earth. Sys. Sci.* 123,1433–1438.
- 913 Bhattacharyya, B., 1967. Tertiary plant fossils from Cherrapunji and Laitryngew in Khasi and  
914 Jainta hills, Assam. *Q. J. Geol. Min. Metall. Soc. India.* 39, 131–134.
- 915 Bhatia H., Srivastava G., Spicer R.A., et al., 2021. Leaf physiognomy records the Miocene  
916 intensification of the south Asia monsoon. *Glob. Planet. Change* 196, 103365.
- 917 Bhatia, H., Srivastava, G., Adhikari, P., et al., 2022. Asian monsoon and vegetation shift:  
918 evidence from the Siwalik succession of India. *Geol. Mag.* 159, 1397–1414.
- 919 Biswas, S.K., Ahuja, A.D., Saproo, M.K., et al., 1976. Geology of Himalayan foot-hills, Bhutan.  
920 In: Cyclostyled Paper Presented at the Himalayan Geology Seminar, New Delhi.
- 921 Bora, D.S., Shukla, U.K., 2005. Petrofacies implication for the lower Siwalik foreland basin  
922 evolution, Kumaun Himalaya, India. *Spec. Pub. Palaeontol. Soc. India* 2, 163–179.
- 923 Boos, W.R., Kuang, Z., 2010. Dominant control of the South Asian monsoon by orographic  
924 insulation versus plateau heating. *Nature* 463, 218–222.
- 925 Brooks, T.M., Mittermeier, R.A., da Fonseca, G.A.B., et al., 2006. Global biodiversity  
926 conservation priorities. *Science* 313, 58–61.
- 927 CEPF., 2005. Ecosystem Profile: Indo-Burman hotspot, eastern Himalayan region. Kathmandu:  
928 WWF, US-Asian Programme /CEPF
- 929 CEPF., 2007. Ecosystem profile: Indo-Burma hotspot, Indo-China region. UK: Critical  
930 ecosystem partnership fund, Birdlife International.

- 931 Chakrabarti, B.K., 2016. Geology of the Himalayan belt deformation, metamorphism,  
932 stratigraphy. Elsevier, pp. 12–46.
- 933 Champion, H.G. Seth, S.K., 1968. A revised survey of the forest types in India. Manager of  
934 Publication, Delhi.
- 935 Chakraborty, T., Taral, S., More, S., et al., 2020. Cenozoic Himalayan foreland basin: An  
936 overview and regional perspective of the evolving sedimentary succession. *Geodynamics*  
937 *of the Indian Plate*. pp. 395–437
- 938 Chatterjee, S., Scotese, C.R., 1999. The breakup of Gondwana and the evolution and  
939 biogeography of Indian plate. *Proc. Natl. Acad. Sci. India* 65A, 397–425.
- 940 Chirouze, F., Dupont-Nivet, G., Huyghe, P., et al., 2012. Magnetostratigraphy of the Neogene  
941 Siwalik group in the far eastern Himalaya: Kameng section, Arunachal Pradesh, India. *J.*  
942 *Asian. Earth. Sci.* 44, 117–135.
- 943 Coutand, I., Barrier, L., Govin, G., et al., 2016. Late Miocene-Pleistocene evolution of India-  
944 Eurasia convergence partitioning between the Bhutan Himalaya and the Shillong Plateau:  
945 new evidences from foreland basin deposits along the Dungsam Chu section, eastern  
946 Bhutan. *Tectonics* 35, 2963–2994.
- 947 Das P., Khan, M.A., De, B., et al., 2007. Evidence of exoparasitic relationship between *Asterina*  
948 (*Asterinaceae*) and *Chonemorpha* (*Apocynaceae*) from the upper Siwalik (Kimin  
949 Formation) sediments of Arunachal sub-Himalaya, India. *J. Mycopathol. Res.* 45, 225–  
950 230.
- 951 Debnath, A., Taral, S., Mullick S., et al., 2021. The Neogene Siwalik succession of the  
952 Arunachal Himalaya: A revised lithostratigraphic classification and its implication for the  
953 regional paleogeography. *J. Geol. Soc. India.* 97, 339–350.

- 954 Ding, L., Spicer, R. A., Yang, J., et al., 2017. Quantifying the rise of the Himalaya orogen and  
955 implications for the south Asian monsoon. *Geology* 45, 215–218.
- 956 Dwivedi, H.D., Prasad, M., Tripathi, P.P., 2006. Angiospermous fossil leaves from the lower  
957 Siwalik sediments of Koilabas area, western Nepal and their significance. *J. Appl. Biol.*  
958 *Sci.* 32, 135–142.
- 959 Farnsworth, A., Lunt, D.J., Robinson, S.A., et al., 2019. Past east Asian monsoon evolution  
960 controlled by paleogeography, not CO<sub>2</sub>. *Sci. Adv.* 5, eaax1697.
- 961 Ferguson, DK., Zetter, R., Paudyal, K.N., 2007. The need for the SEM in palaeopalynology.  
962 *Comptes Rendus Palevol.* 6, 423–430.
- 963 Fick, S.E., Hijmans, R.J., 2017. WorldClim2: new 1-km spatial resolution climate surfaces for  
964 global land surfaces. *Int. J. Climatol.* 37, 4302–4315.
- 965 Grierson, A.J.C., Long, D.G., 1983. *Flora of Bhutan*. Vol. 1. Royal botanical garden, Edinburgh.
- 966 Ganguly, S., Rao, D.P., 1970. Stratigraphy and structure of the Tertiary foothills of eastern  
967 Himalaya. Darjeeling district. *West Bengal Quart. J. Geol. Min. Metal. Soc. India* 42,  
968 185–195.
- 969 Guleria, J.S., 1992. Neogene vegetation of peninsular India. *Palaeobotanist* 40, 285–311.
- 970 Harris, I., Jones, P.D., Osborn, T.J., et al., 2014. Updated high-resolution grids of monthly  
971 climatic observations – the CRU TS3.10 Dataset. *Int. J. Climatol.* 34, 623–642.
- 972 Hazra P.K., Verma, D.M., Giri, G.S., 1996. *Materials for the flora of Arunachal Pradesh*, vol 1  
973 *Bot. Sur. India*. Calcutta.
- 974 Huffaker, C.B., 1942. Vegetational correlations with vapour pressure deficit and relative  
975 humidity. *Am. Midl. Nat.* 28, 486–500.
- 976 Huggett, R.J., 2004. *Fundamentals of Biogeography*. Routledge, New York, USA.

- 977 Johnson, N.M., Stix, J., Tauxe, L., et al., 1985. Paleomagnetic chronology, fluvial processes, and  
978 tectonic implications of the Siwalik deposits near Chinji village, Pakistan. *J. Geol.* 93,  
979 27–40.
- 980 Joshi, A., Mehrotra, R.C., 2003. A thelypteridaceous fossil fern from the lower Siwalik of the  
981 east Kameng district, Arunachal Pradesh, India. *J. Geol. Soc. India* 61, 483–486.
- 982 Joshi, A., Mehrotra, R.C., De, A., 2003a. A fossil wood from the Upper Siwalik sediments of  
983 West Kameng District, Arunachal Pradesh, India. *Proc. Fourth South Asia Geological*  
984 *Congress (GEOSAS - IV), The Director General Geol. Surv. India, Kolkata, pp. 312–315.*
- 985 Joshi, A., Tewari, R., Mehrotra, R.C., et al., 2003b. Plant remains from the Upper Siwalik  
986 sediments of West Kameng District, Arunachal Pradesh, India. *J. Geol. Soc. India* 61, 319–  
987 324.
- 988 Joshi, A., Mehrotra, R.C., 2007. Mega remains from the Siwalik sediments of west and east  
989 Kameng Districts, Arunachal Pradesh. *J. Geol. Soc. India* 69, 1256–1266.
- 990 Karunakaran, C., Ranga Rao, A., 1976. Status of exploration for the Hydrocarbons in the  
991 Himalayan region-contributions to the stratigraphy and structure. In: *International*  
992 *Himalayan Geological Seminar India. Section III, O. N. G. C, pp. 1–72.*
- 993 Kaul, R.N., Haridasan, K., 1987. Forest type of Arunachal Pradesh- a preliminary study. *J. Econ.*  
994 *Taxon. Bot.* 9, 379–389.
- 995 Khan, M.A., Bera, S., 2007. *Dysoxylum miocostulatum* sp. nov. -a fossil leaflet of Meliaceae  
996 from the lower Siwalik sediments of west Kameng district, Arunachal Pradesh, eastern  
997 India. *Indian. J. Geol.* 79, 63–68.
- 998 Khan, M.A., Bera, S., 2010. Record of fossil fruit wing of *Shorea* Roxb. from the Neogene of  
999 Arunachal Pradesh. *Curr. Sci.* 98, 1573–1574.

- 1000 Khan, M.A., Bera, S., 2012. *Glochidion palaeogamblei* sp. nov. – a new fossil leaf of  
1001 Euphorbiaceae from the Pliocene sediments of Arunachal Pradesh, eastern India and its  
1002 palaeoclimatic significance. Diversity and conservation of plants and traditional  
1003 knowledge Bishen Singh Mahendra Pal Singh, Dehradun, pp. 149–154.
- 1004 Khan, M.A., Bera, S., 2014a. On some Fabaceous fruits from the Siwalik sediments (Middle  
1005 Miocene–Lower Pleistocene) of eastern Himalaya. J. Geol. Soc. India 83, 165–174.
- 1006 Khan, M.A., Bera, S., 2014b. New lauraceous species from the Siwalik Forest of Arunachal  
1007 Pradesh, eastern Himalaya, and their palaeoclimatic and palaeogeographic implications.  
1008 Turk. J. Bot. 38, 453–464.
- 1009 Khan, M. A., Bera, S., 2016b. Occurrence of *Persea* Mill. from the Siwalik Forest of Darjeeling,  
1010 eastern Himalaya: paleoclimatic and paleogeographic implications. J. Earth Sci. 27, 882–  
1011 889.
- 1012 Khan, M. A., Bera, S., 2016b. Occurrence of *Persea* Mill. From the Siwalik Forest of Darjeeling,  
1013 eastern Himalaya: paleoclimatic and paleogeographic implications. J. Earth Sci. 27, 882–  
1014 889.
- 1015 Khan, M. A., Bera, S., 2017. First discovery of fossil winged seeds of *Pinus* L. (family Pinaceae)  
1016 from the Indian Cenozoic and its paleobiogeographic significance. J. Earth Sci. 126, 1–  
1017 11.
- 1018 Khan, M.A., De, B., Bera, S., 2007. A fossil fern-leaflet of family Thelypteridaceae from the  
1019 Middle Siwalik sediments of West Kameng district, Arunachal Pradesh. J. Bot. Soc.  
1020 Bengal 61, 65–69.
- 1021 Khan, M.A., De, B., Bera, S., 2008. Fossil leaves resembling modern *Terminalia chebula*  
1022 Retzius from the lower Siwalik sediments of Arunachal Pradesh, India. Pleione 2, 38–41.

- 1023 Khan, M.A., De, B., Bera, S., 2009. Leaf-impressions of *Calophyllum* L. from the middle  
1024 Siwalik sediments of Arunachal sub-Himalaya, India. *Pleione* 3, 101–106.
- 1025 Khan, M.A., Ghosh, R., Bera, S., et al., 2011. Floral diversity during Plio-Pleistocene Siwalik  
1026 sedimentation (Kimin Formation) in Arunachal Pradesh, India, and its palaeoclimatic  
1027 significance. *Palaeodivers. Palaeoenvir.* 91, 237–255.
- 1028 Khan, M.A., Spicer, R.A., Bera, S., et al., 2014a. Miocene to Pleistocene floras and climate of  
1029 the eastern Himalayan Siwaliks, and new palaeoelevation estimates for the Namling-  
1030 Oiyug Basin, Tibet. *Glob. Planet. Change* 113, 1–10.
- 1031 Khan, M.A., Spicer, R.A., Spicer, T. E.V., et al., 2014b. Fossil evidence of insect folivory in the  
1032 eastern Himalayan Neogene Siwalik forests. *Palaeogeogra. Palaeoclimatol. Palaeoecol.*  
1033 410, 264–277.
- 1034 Khan, M.A., Spicer, T.E.V., Spicer, R.A., et al., 2014c. Occurrence of *Gynocardia odorata*  
1035 Robert Brown (Achariaceae, formerly Flacourtiaceae) from the Plio-Pleistocene  
1036 sediments of Arunachal Pradesh, northeast India and its palaeoclimatic and  
1037 phytogeographic significance. *Rev. Palaeobot. Palynol.* 211, 1–9.
- 1038 Khan, M.A., Bera, S., Ghosh, R., et al., 2015a. Leaf cuticular morphology of some angiosperm  
1039 taxa from the Siwalik sediments (middle Miocene to lower Pleistocene) of Arunachal  
1040 Pradesh, eastern Himalaya: Systematic and palaeoclimatic implications. *Rev. Palaeobot.*  
1041 *Palynol.* 214, 9–26.
- 1042 Khan, M.A., Bera, S., Spicer, R.A., et al., 2015b. Plant–arthropod associations from the Siwalik  
1043 forests (middle Miocene) of Darjeeling sub-Himalaya, India. *Palaeogeogr.*  
1044 *Palaeoclimatol. Palaeoecol.* 438, 191–202.



- 1045 Khan, M.A., Spicer, R.A., Spicer, T.E.V., et al., 2016. Occurrence of *Shorea* Roxburgh ex C.F.  
1046 Gaertner (Dipterocarpaceae) in the Neogene Siwalik forests of eastern Himalaya and its  
1047 Biogeography during the Cenozoic of Southeast Asia. *Rev. Palaeobot. Palynol.* 233, 236–  
1048 254.
- 1049 Khan, M.A., Spicer, R.A., Spicer, T. E. V., et al., 2017a. Evidence for diversification of  
1050 *Calophyllum* L. (Calophyllaceae) in the Neogene Siwalik forests of eastern Himalaya.  
1051 *Plant Syst. Evol.* 303, 371–386.
- 1052 Khan, M.A., Spicer, R.A., Spicer, T.E.V., et al., 2017b. First occurrence of *Mastixioid*  
1053 (Cornaceae) fossil in India and its biogeographic implication. *Rev. Palaeobot. Palynol.*  
1054 247, 83–96.
- 1055 Khan M.A., Bera, M., Spicer, R.A., et al., 2018a. Evidence of simultaneous occurrence of tylosis  
1056 formation and fungal interaction in a late Cenozoic angiosperm from the eastern  
1057 Himalaya. *Rev. Palaeobot. Palynol.* 259, 171–184.
- 1058 Khan M.A., Bera, M., Bera, S., 2018b. *Vizellopsidites siwalika*, a new fossil epiphyllous fungus  
1059 from the Plio-Pleistocene of Arunachal Pradesh, eastern Himalaya. *Nova Hedwigia* 107,  
1060 543–555.
- 1061 Khan, M. A., Bera, M., Spicer, R.A., et al., 2019a. Floral diversity and environment during the  
1062 middle Siwalik sedimentation (Pliocene) in the Arunachal sub-Himalaya. *Paleobiodivers.*  
1063 *Paleoenviron.* 99, 401–424.
- 1064 Khan, M. A., Bera, M., Spicer, R. A., et al., 2019b. Palaeoclimatic estimates for a latest  
1065 Miocene-Pliocene flora from the Siwalik group of Bhutan: evidence for the development  
1066 of the south Asian monsoon in the eastern Himalaya. *Palaeogeogra. Palaeoclimatol.*  
1067 *Palaeoecol.* 514, 326–335.

- 1068 Khan, M.A., Bera, M., Bera, S., 2019c. A new meliolaceos foliicolous fungus from the Plio-  
1069 Pleistocene of Arunachal Pradesh, eastern Himalaya. *Rev. Palaeobot. Palynol.* 268, 55–  
1070 64.
- 1071 Kovach, W.L., Spicer, R.A., 1996. Canonical correspondence analysis of leaf physiognomy: a  
1072 contribution to the development of a new palaeoclimatological tool. *Palaeoclimates* 2,  
1073 125–38.
- 1074 Kumar, G., 1997. *Geology of the Arunachal Pradesh*. Geological Society of India, Bangalore.
- 1075 Lakhanpal, R.N., 1965. Occurrence of *Zizyphus* in the Siwaliks near Jawalamukhi. *Curr. Sci.* 34,  
1076 666–667.
- 1077 Lakhanpal, R.N., 1967. Fossil Rhamnaceae from the lower Siwalik beds near Jawalamukhi,  
1078 Himachal Pradesh. Publication of Centre of Advance Study in Geology, Panjab  
1079 University, Chandigarh 3, 23–26.
- 1080 Lakhanpal, R.N., 1970. Tertiary floras of India and their bearing on the historical geology of the  
1081 region. *Taxon* 19, 675–694.
- 1082 Lakhanpal, R.N., Awasthi, N., 1992. New species of *Fissistigma* and *Terminalia* from the  
1083 Siwalik sediments of Balugoloa, Himachal Pradesh. *Geophytology* 21, 49–52.
- 1084 Mandal, A., Samajpati, N., Bera, S., 2009. In situ occurrence of epiphyllous fungus *Phomites*  
1085 *Fritel* from the lower Siwalik sediments of Darjeeling foothills. *J. Bot. Soc. Bengal* 63,  
1086 37–40.
- 1087 Mandal, A., Samajpati, N., Bera, S., 2011. A new species of *Meliolinites* (fossil Meliolales) from  
1088 the Neogene sediments of sub-Himalayan West Bengal, India. *Nova Hedwigia* 92, 435–  
1089 440.

- 1090 Medlicott, H.B., 1865. The coal of Assam, results of a brief visit to the coalfields that province in  
1091 1865; with geological note on Assam and the hills to the south of it. *Memoirs of Geol.*  
1092 *Sur. India* 4, 388–442.
- 1093 Mehrotra, R.C., 2000a. Study of plant megafossils from the Tura Formation of Nangwabibra,  
1094 Garo Hills, Meghalaya. *Palaeobotanist* 49, 225–237.
- 1095 Mehrotra, R.C., 2000b. Two new fossils fruits from the Oligocene sediments of Makum  
1096 coalfield, Assam, India. *Curr. Sci.* 79, 1482–1483.
- 1097 Mehrotra R.C., Awasthi N., Dutta S.K., 1999. Study of fossil wood from the upper Tertiary  
1098 sediments (Siwalik) of Arunachal Pradesh, India and its implication in palaeoecological  
1099 and phytogeographical interpretations. *Rev. Palaeobot. Palynol.* 107, 223–247.
- 1100 Mehrotra, R.C., Srivastava, G., Srikarni, C., 2018. *Lagerstroemia* L. wood from the Kimin  
1101 Formation (upper Siwalik) of Arunachal Pradesh and its climatic and phytogeographic  
1102 significance. *J. Geol. Soc. India* 91, 695–699.
- 1103 Mitra, S., Banerjee, M., 2000. On the occurrence of epiphyllous Deuteromycetous fossil fungi  
1104 *Palaeocercospora siwalikensis* gen. et. sp. nov. and *Palaeocolletotrichum graminoides*  
1105 gen. et. sp. nov. from Neogene sediments of Darjeeling foothills, Eastern Himalaya. *J.*  
1106 *Mycopathol. Res.* 37, 7–11.
- 1107 Mitra, S., Banerjee, M., 2004. Fossil fruit *Derrisocarpon miocenicum* gen. et. sp. nov. and leaflet  
1108 *Derrisophyllum Siwalicum* gen. et. sp. nov. cf. *Derris trifoliata* Lour. of Fabaceae from  
1109 Siwalik sediments of Darjeeling foothills, eastern Himalaya, India with remarks on site of  
1110 origin and distribution of the genus. *Phytomorphology* 54, 253–263.

- 1111 Mitra S., Bera, S., Banerjee, M., 2002. On a new epiphyllous fungus *Palaeoasterina siwalika*  
1112 gen. et. sp. nov. from the Siwalik (middle Miocene) sediments of Darjeeling foothills,  
1113 India with remarks on environment. *Phytomorphology* 52, 285–292.
- 1114 Molnar, P., Boos, W.R., Battisti, D.S., 2010. Orographic controls on climate and paleoclimate of  
1115 Asia: thermal and mechanical roles for the Tibetan Plateau. *Annu. Rev. Earth Planet. Sci.*  
1116 38, 77–102.
- 1117 Morley, R.J., 2000. Origin and evolution of tropical rain forests. Chichester, UK, p. 27.
- 1118 More, S., Rit, R., Khan, M.A., et al., 2018. Record of Leaf and Pollen cf. *Sloanea*  
1119 (Elaeocarpaceae) from the Middle Siwalik of Darjeeling sub-Himalaya, India and its  
1120 Palaeobiogeographic Implications. *J. Geol. Soc. India* 91, 301–306.
- 1121 Mosbrugger, V., Utescher, T., 1997. The coexistence approach—a method for quantitative  
1122 reconstructions of Tertiary terrestrial palaeoclimate data using plant fossils. *Palaeogeogr.*  
1123 *Palaeoclimatol. Palaeoecol.* 134, 61–86.
- 1124 Mosbrugger, V., 1999. The nearest living relative method. In fossil plants and spores: Modern  
1125 techniques (eds TP Jones and NP Rowe). Bath: Geol. Soc. London, pp. 261–265.
- 1126 Mosbrugger, V., Utescher, T., Dilcher, D.L., 2005. Cenozoic continental climatic evolution of  
1127 Central Europe. *Proc. Natl. Acad. Sci. U.S.A.* 102, 14964–14969.
- 1128 New, M., Hulme, M., Jones, P., 1999. Representing Twentieth-Century Space–Time Climate  
1129 Variability. Part I: Development of a 1961–90 Mean Monthly Terrestrial Climatology. *J.*  
1130 *Clim.* 12, 829–856.
- 1131 New, M., Lister, D., Hulme, M., et al., 2002. A high-resolution data set of surface climate over  
1132 global land areas. *Clim. Res.* 21, 1–15.

- 1133 Pathak, N.R., 1969. Megafossils from the foothills of Darjeeling district, India. J. Bot. Soc.  
1134 Bengal, Calcutta, pp. 379–386.
- 1135 Parkash, B., Sharma, R.P., Roy, A.K., 1980. The Siwalik group (Molasse) sediments shed by  
1136 collision of continental plates. Sediment. Geol. 25, 127–159.
- 1137 Pilgrim, G.E., 1910. Preliminary note on a revised classification of the Tertiary freshwater  
1138 deposits of India. Records of the geological survey of India, vol XL, Part 3, pp. 185–205.
- 1139 Pilgrim, G.E., 1913. The correlation of the Siwaliks with mammal horizons of Europe. Rec.  
1140 Geol. Sur. India 43, 264–326.
- 1141 Pradhan, U.C., Lachungpa, S.T., 1990. Sikkim-Himalayan *Rhododendron*. Primulaceae Books,  
1142 Kalimpong, Darjeeling, p. 130.
- 1143 Prasad, M., 1990. Fossil flora from the Siwalik sediments of Koilabas, Nepal. Geohydrology 19,  
1144 79–105.
- 1145 Prasad, M., 1994a. Siwalik (middle-Miocene) leaf impressions from the foot hills of the  
1146 Himalaya, India. Ter. Res.15, 53–90.
- 1147 Prasad, M., 1994b. Plant megafossils from the Siwalik sediments of Koilabas, central Himalaya,  
1148 Nepal and their impact on palaeoenvironment. Palaeobotanist 42, 126–156.
- 1149 Prasad, M., 2006. Plant fossils from Siwalik sediments of Himachal Pradesh and their  
1150 palaeoclimatic significance. Phytomorphology 56, 9–22.
- 1151 Prasad, M., 2008. Angiospermous fossil leaves from the Siwalik foreland and their paleoclimatic  
1152 implication. Paleobotanist 57, 177–215.
- 1153 Prakash, U., Prasad, M., 1984. Wood of *Bauhinia* from the lower Siwalik beds of Uttar Pradesh,  
1154 India. Paleobotanist 32, 140–145.

- 1155 Prasad, M., Kannaujia, A.K., Alok, Singh, S.K., 2015. Plant megaf flora from the Siwalik (upper  
1156 Miocene) of Darjeeling district, West Bengal, India and its palaeoclimatic and  
1157 phytogeographic significance. *Palaeobotanist* 64, 13–94.
- 1158 Prasad, M., Dwivedi, H.D., 2007. Systematic study of the leaf impressions from the Churia  
1159 Formation of Koilabas area, Nepal and their significance. *Palaeobotanist* 56, 39–54.
- 1160 Prasad, M., Antal, J.S., Tiwari, V.D., 1997. Investigation on plant fossil from Seria Naka in the  
1161 Himalayan foot hills of Uttar Pradesh, India. *Paleobotanist* 46, 13–30.
- 1162 Prasad, M., Antal, J.S., Tripathi, P.P., et al., 1999. Further contribution to the Siwalik flora from  
1163 the Koilabas area, western Nepal. *Palaeobotanist* 48, 49–95.
- 1164 Prasad, M., Tripathi, P.P., 2000. Plant megafossils from the Siwalik sediments of Bhutan and  
1165 their climatic significance. *Biol. Mem.* 26, 6–19.
- 1166 Prasad, M., Ghosh, R., Tripathi, P.P., 2004. Floristic and climate during the Siwalik (middle  
1167 Miocene) near Kathgodam in the Himalayan foothills of Uttaranchal, India. *J. Palaeontol.*  
1168 *Soc. India.* 49, 35–93.
- 1169 Ranga Rao, A., Venkatechala, B.S., Sastri, V.V., 1979. Neogene/Quaternary boundary and the  
1170 Siwalik. In: Sastri, V.V.e.a. (Ed.), *Field Conference on Neogene–Quaternary Boundary,*  
1171 *India.*
- 1172 Ranga Rao, A., Agarwal, R.P., Sharma, U.N., et al., 1988. Magnetic polarity stratigraphy and  
1173 vertebrate palaeontology of the upper Siwalik subgroup of Jammu Hills, India. *J. Geol.*  
1174 *Soc. India* 31, 361–385.
- 1175 Sahni, B., 1964a. *Revision of Indian Fossil Plants-Monocotyledons. Monograph 1.* Birbal Sahni  
1176 *Institute of Palaeobotany, Lucknow.*

- 1177 Sahni, B., 1964b. Revision of Indian Fossil Plants-part III. Monocotyledons. Monograph 1.  
1178 Birbal Sahni Institute of Palaeobotany, Lucknow.
- 1179 Shashi, Pandey, S.M., Tripathi, P.P., 2006. Fossil leaf impressions from Siwalik sediments of  
1180 Himalayan foot hills of Uttaranchal, India and their significance. *Palaeobotanist* 55, 77–  
1181 87.
- 1182 Shashi, Pandey, S.M., Tripathi, P.P., 2008. Siwalik (middle Miocene) leaf impressions from  
1183 Tanakpur area, Uttaranchal and their bearing on climate. *Geophytology* 37, 99–108.
- 1184 Singh, G., 1975. On the discovery of first vertebrate fossil from the Upper Tertiary of Subansiri  
1185 district, Arunachal Pradesh. *Indian Min.* 29, 65–67.
- 1186 Singh, T., 1983. On the stratigraphic correlation of upper Tertiary of Arunachal Pradesh. *Geol.*  
1187 *Sur. India Mis. Publ.* 43, 82–84.
- 1188 Singh, T., 2007. Geology of Itanagar capital complex, Arunachal Himalaya, with special  
1189 reference to neotectonics. *J. Geol. Soc. India* 70, 339–352.
- 1190 Singh, T., Prakash, U., 1980. Leaf-impressions from the Siwalik sediments of Arunachal  
1191 Pradesh. *Geohydrology* 10, 104–107.
- 1192 Spicer, R. A., 1991. Plant Taphonomic Processes. In: Allison, P.A., Briggs, D.E.G., *Taphonomy:*  
1193 *Releasing the Data Locked in the Fossil Record.* Plenum Press, New York, pp. 71–113.
- 1194 Spicer, R.A., Herman, A.B., 2010. The Late Cretaceous environment of the Arctic: a quantitative  
1195 reassessment using plant fossils. *Palaeogeogr. Palaeoclimatol. Palaeoecol.* 295, 423–42.
- 1196 Spicer, R.A., Valdes, P.J., Hughes, A.C., et al., 2019. New insights into the thermal regime and  
1197 hydrodynamics of the early Late Cretaceous Arctic. *Geol. Mag.* 157, 1729–1749.
- 1198 Spicer, R.A., Wolfe, J.A., 1987. Plant taphonomy of late Holocene deposits in Trinity (Clair  
1199 Engle) Lake, northern California. *Paleobiology* 13, 227–245.

- 1200 Spicer, R.A., Yang, J., Spicer, T.E.V., et al., 2021. Woody dicot leaf traits as a palaeoclimate  
1201 proxy: 100 years of development and application. *Palaeogeogr. Palaeoclimatol.*  
1202 *Palaeoecol.* 562, 110138
- 1203 Srivastava, R., Mehrotra, R.C., 2009. Plant fossils from Dafla Formation, west Kameng district,  
1204 Arunachal Pradesh. *Palaeobotanist* 58, 33–49.
- 1205 Srivastava, G., Gaur, R., Mehrotra, R.C., 2015. *Lagerstroemia* L. from the middle Miocene  
1206 Siwalik deposits, northern India: Implication for Cenozoic range shifts of the genus and  
1207 the family Lythraceae. *J. Earth. Syst. Sci.* 124, 227–239.
- 1208 Srivastava, G., Mehrotra, R.C., Sirkarni, C., 2018. Fossil wood flora from the Siwalik group of  
1209 Arunachal Pradesh, India and its climatic and phytogeographic significance. *J. Earth.*  
1210 *Syst. Sci.* 127, 1–22.
- 1211 Srivastava, G., Farnsworth, A., Bhatia, H., et al., 2021. Climate and vegetation change during the  
1212 upper Siwalik—a study based on the palaeobotanical record of the eastern Himalaya.  
1213 *Paleobiodivers. Paleoenviron.* 101, 103–121.
- 1214 Sundriyal, M., 1999. ‘Distribution, Propagation and Nutritive Value of Some Wild Edible Plants  
1215 in the Sikkim Himalaya.’ PhD Thesis, High Altitude Plant Physiology Research Centre,  
1216 HNB Garjhwali University, Srinagar (Garhwal) and GB Pant Institute of Himalayan  
1217 Environment and Development, Sikkim Unit, Sikkim, India
- 1218 Su, T., Liu, Y.S., Jacques, F.M.B., et al., 2013. The intensification of the east Asian winter  
1219 monsoon contributed to the disappearance of *Cedrus* (Pinaceae) in southwestern China.  
1220 *Quat. Res.* 80, 316–325.
- 1221 Takhtajan, A. 1969 *Flowering Plants: Origin and Dispersal*. Edinburgh: Oliver & Boyd.



- 1222 Tang, Q., Zhang, X., Yang, X., et al., 2013. Cold winter extremes in northern continents linked  
1223 to Arctic Sea ice loss. *Environ. Res. Lett.* 8, 014036.
- 1224 Tang, H., Eronen, J. T., Kaakinen, A., et al., 2015. Strong winter monsoon wind causes surface  
1225 cooling over India and China in the Late Miocene. *Clim. Past* 11. 63–93.
- 1226 Taral, S., Kar, N., Chakrobarty, T., 2017. Wave-generated structures in the Siwalik rocks of Tista  
1227 valley, eastern Himalaya: Implication for regional palaeogeography. *Curr. Sci.* 113, 887–  
1228 901.
- 1229 Taral, S., Chakraborty, T., Huyghe, P., et al., 2019. Shallow marine to fluvial transition in the  
1230 Siwalik succession of the Kameng River section, Arunachal Himalaya and its implication  
1231 for foreland basin evolution. *J. Asian. Earth. Sci.* 184: 103980.
- 1232 Teodoridis, V., Kovar-Eder, J., Marek, P., et al., 2011. The integrated plant record vegetation  
1233 analysis: Internet platform and online application. *Acta Musei Nationalis Pragae, Series*  
1234 *B–Historia Naturalis.* 67, 159–164.
- 1235 ter Braak, C.J.F., 1986. Canonical correspondence analysis: a new eigenvector technique for  
1236 multivariate direct gradient analysis. *Ecology* 67, 1167–1179.
- 1237 Thanukos, Anna 2012. “*Uniformitarianism: Charles Lyell*” University of California Museum of  
1238 Paleontology. Retrieved 23 July 2012.
- 1239 Tripathi, P.P., Pandey, P., Mishra, R.K., 2007. Leaf impressions from the Siwalik beds of south-  
1240 eastern Bhutan and their climatic significance. *Plant Archives* 7, 169–173.
- 1241 Tripathi, P.P., Pandey, S.M., Prasad, M., 2002. Angiospermous leaf impressions from Siwalik  
1242 sediments of Himalayan foot hills near Jarva, U.P. and their bearing on palaeoclimate.  
1243 *Biol. Mem.* 28, 79–90.

- 1244 Utescher, T., Bruch, A. A., Erdei, B., et al., 2014. The Coexistence Approach – Theoretical  
1245 background and practical considerations of using plant fossils for climate quantification,  
1246 *Palaeogeogr. Palaeoclimatol. Palaeoecol.* 410, 58–73.
- 1247 Yang, J., Spicer, R.A., Spicer, T.E.V., Li, C.S., 2011. ‘CLAMP online’: a new web-based  
1248 palaeoclimate tool and its application to the terrestrial Paleogene and Neogene of North  
1249 America. *Palaeobiol. Palaeoenvir.* 91, 163–183.
- 1250 Yang, J., Spicer, R.A., Spicer, T.E.V., et al., 2015. Leaf form-climate relationships on the global  
1251 stage: an ensemble of characters. *Glob. Ecol. Biogeogr.* 10, 1113–1125.
- 1252 WWF ICIMOD, 2001. Ecoregion-based conservation in the eastern Himalaya: identifying  
1253 important areas for biodiversity conservation. Kathmandu: WWF-Nepal.
- 1254 Wolfe, J.A., 1993. A method of obtaining climatic parameters from leaf assemblages. *Geol. Soc.*  
1255 *Am. Bull.* 2040, 1–73.
- 1256 Valdiya, K.S., 2002. Emergence and evolution of Himalaya: reconstructing history in the light of  
1257 recent studies. *Prog. Phys. Geogr.* 26, 360–399.
- 1258 Varma, C.P., 1968. On a collection of leaf-impressions from Hardwar, Uttar Pradesh. *J.*  
1259 *Palaeontol. Soc. India* 5-9, 92–88.
- 1260 Vishnu (née Mandal) A., Khan, M.A., Bera, M., et al., 2017. Fossil Asterinaceae in the  
1261 phyllosphere of the eastern Himalayan Neogene Siwalik Forest and their palaeoecological  
1262 significance. *Bot. J. Linn. Soc.* 185, 147–167.
- 1263 Vishnu, A., Khan, M.A., Bera, M., et al., 2019. Occurrence of *Phoma* Sacc. in the phyllosphere  
1264 of Neogene Siwalik Forest of Arunachal sub-Himalaya and its palaeoecological  
1265 implications. *Fungal Biol.* 123, 18–28.

1266 Zachos, J.C., Dickens, G.R., Zeebe, R.E., 2008. An early Cenozoic perspective on greenhouse  
1267 warming and carbon-cycle dynamics. *Nature* 451, 279–283.

1268 Zachos J.C., Pagani, M., Sloan, L., et al., 2001. Trends, rhythms, and aberrations in global  
1269 climate 65 Ma to present. *Science* 292, 686–693.

1270

## 1271 **Table captions**

1272 **Table 1.** A generalised lithostratigraphy of Siwalik sediments in the eastern Himalayas (*modified*  
1273 *after* Khan et al., 2014a, 2019b; Taral et al., 2017).

1274 **Table 2.** A checklist of megafossil plant remains of Siwalik of the eastern Himalayas.

1275 **Table 3.** Summary of temperature-related CLAMP-derived metrics for Siwalik leaf assemblages  
1276 from the eastern Himalayas. Values obtained by a CLAMP calibration based on PhysgAsia2 trait  
1277 scores and WorldClim2 climate data as well as HiResGridMetAsia2 (in parentheses) gridded  
1278 climate data. MAT – mean annual temperature; WMMT – warm month mean temperature;  
1279 CMMT – cold month mean temperature; MIN\_T\_W – minimum temperature of the warmest  
1280 month; MAX\_T\_C – maximum temperature of the coldest month; THERM. – compensated  
1281 thermicity index: sum of mean annual temp., min. temp. of coldest month, max. temp. of coldest  
1282 month,  $\times 10$ , with compensations for better comparability across the globe; GDD\_0 – sum of  
1283 mean monthly temperature for months with mean temperature greater than 0 °C multiplied by  
1284 number of days; GDD\_5 – sum of mean monthly temperature for months with mean temperature  
1285 greater than 5 °C multiplied by number of days and LGS – length of the growing season when  
1286 mean temperatures are above 10 °C

1287 **Table 4.** Summary of precipitation and moist enthalpy CLAMP-derived metrics for Siwalik leaf  
1288 assemblages from the eastern Himalayas. Values obtained by a CLAMP calibration based on

1289 PhysgAsia2 trait scores and WorldClim2 climate data as well as HiResGridMetAsia2 gridded  
1290 climate data, in parentheses. GSP – precipitation during the growing season; MMGSP – mean  
1291 monthly precipitation during the growing season; 3WET – precipitation during the three  
1292 consecutive wettest months; 3DRY – precipitation during the three consecutive driest months;  
1293 ENTH – annual mean moist enthalpy.

1294 **Table 5.** Summary of humidity CLAMP-derived metrics for Siwalik leaf assemblages from the  
1295 eastern Himalayas. Values obtained by a CLAMP calibration based on PhysgAsia2 trait scores  
1296 and WorldClim2 climate data as well as HiResGridMetAsia2 (in parentheses) gridded climate  
1297 data. RH. ANNUAL – annual mean relative humidity; SH. ANNUAL – annual mean specific  
1298 humidity; VPD.ANN – annual mean vapour pressure deficit; VPD.SUM – mean VPD for the  
1299 summer quarter; VPD.WIN – mean VPD for the winter quarter; VPD.SPR – mean VPD for the  
1300 spring quarter; VPD-AUT – mean VPD for the autumn quarter; PET.ANN – annual mean  
1301 potential evapotranspiration; PET.WARM – mean potential evapotranspiration for the warmest  
1302 quarter; PET.COLD – mean potential evapotranspiration for the coldest quarter.

1303

#### 1304 **Figure captions**

1305 **Figure 1.** Maps showing the seven sectors of the Siwalik belt (modified after Karunakaran and  
1306 Ranga Rao, 1976) showing the locations of the present study areas

1307 **Figure 2.** a-c. Fossiliferous Siwalik exposures of the eastern Himalayas (a: Darjeeling; b:  
1308 Bhutan; c: Southeastern Himalaya)

1309 **Figure 3.** (a) A fossil leaflet of *Dysoxylum miocostulatum* Khan and Bera (2007) from Lower  
1310 Siwalik sediments of Southeastern Himalaya (CUH/PPL/P26) (Scale bar = 1 cm); (b, c) Winged  
1311 seeds of *Pinus arunachalensis* Khan and Bera (2017) from Lower Siwalik sediments of

1312 Southeastern Himalaya (CUH/PPL/P/f/61a, b) (Scale bar = 1 cm); (d) A fossil leaf *Quercus* cf.  
 1313 *lamellosa* Khan et al. (2011) from Upper Siwalik sediments of Southeastern Himalaya  
 1314 (CUH/PPL/IB7/46) (Scale bar = 1 cm); (e) *Dysoxylum raptiensis* Khan et al. (2015a) from Upper  
 1315 Siwalik sediments of Southeastern Himalaya (CUH/PPL/IB7/17) – abaxial cuticle showing  
 1316 stomata and epidermal cells (Scale bar = 10 µm); (f) Fossil leaf of *Shorea mioobtusa* Khan et al.  
 1317 (2016) from Lower Siwalik sediments of Southeastern Himalaya (CUH/PPL/ P 83) (Scale Bar =  
 1318 1 cm); (g) *Dipterocarpus koilabasensis* Khan et al. (2015a) from Upper Siwalik sediments of  
 1319 Southeastern Himalaya (CUH/PPL/IB7/3) - abaxial cuticle, hyphae with opposite and pointed  
 1320 appressoria of epiphyllous fungi *Asterina* sp. (Scale bar = 10 µm); (h) *Calophylloxylon*  
 1321 *eoinophyllum* Khan et al. (2017a) from Upper Siwalik sediments of Southeastern Himalaya  
 1322 (CUH/PPL/IB7/W1A) - transverse section (T.S.) showing diffuse vessel distribution and solitary  
 1323 arrangement, and parenchyma bands (Scale bar = 10 µm); (i) Fossil fruit wing of *Shorea*  
 1324 *mioassamica* Khan and Bera (2010) from Lower Siwalik sediments of Southeastern Himalaya  
 1325 (CUH/PPL/P14) (Scale bar = 1 cm)

1326 **Figure 4.** (a) A fossil leaf of *Actinodaphne palaeoangustifolia* Khan et al. (2011) from Upper  
 1327 Siwalik sediments of Southeastern Himalaya (CUH/PPL/IB7/40) (Scale bar = 1 cm); (b) A fossil  
 1328 leaf of *Calophyllum suraikholaensis* Khan et al. (2009) from Middle Siwalik sediments of  
 1329 Southeastern Himalaya (CUH/PPL/B1) (Scale bar = 1 cm); (c) Light micrographs of *Gmelina*  
 1330 *siwalika* Khan et al. (2018a) from Upper Siwalik sediments of Southeastern Himalaya  
 1331 (CUH/PPL/C<sub>3</sub>/44) - tangential longitudinal sections of the secondary xylem showing 2–3 seriate  
 1332 ray cells (Scale bar = 50 µm); (d) *Gynocardia arunachalensis* Khan et al. (2014c) from Upper  
 1333 Siwalik sediments of Southeastern Himalaya (CUH/PPL/IB7/f/61a) - fossil seed showing thick,  
 1334 leathery seed coat (Scale bar =1 cm); (e) Fossil leaf of *Glochidion siwalikum* Khan et al. (2019a)

1335 from Middle Siwalik sediments of Southeastern Himalaya (CUH/PPL/B/64A) (Scale bar = 1  
1336 cm); (f) *Cyathea siwalika* Bera et al. (2014) from Upper Siwalik sediments of Southeastern  
1337 Himalaya (CUH/PPL/IB7/TF/1) - Cyatheoid arrangement of vascular bundles within the leaf  
1338 scar (scale bar = 1 cm); (g) *Calophyllum suraikholaensis* Khan et al. (2015a) from Upper Siwalik  
1339 sediments of Southeastern Himalaya (CUH/PPL/IB7/19) - lower cuticle showing paracytic  
1340 stomata and epidermal cells (Scale bar = 10  $\mu$ m).

1341 **Figure 5.** (a) A fossil leaf of *Persea preglaucescens* Khan and Bera (2014) from Middle Siwalik  
1342 sediments of Southeastern Himalaya (CUH/PPL/B/19) (Scale bar = 1 cm); (b) A well-preserved  
1343 wing-like persistent calyx lobe of *Shorea bhalukpongensis* Khan et al. (2016) from Middle  
1344 Siwalik sediments of Southeastern Himalaya (CUH/PPL/B/f/19) showing characteristic parallel  
1345 primary veins (green arrows) (Scale bar = 1 cm); (c) Light micrographs of *Meliolinites*  
1346 *neogenicus* Khan et al. (2019c) from Upper Siwalik sediments of Southeastern Himalaya  
1347 (CUH/PPL/IB7/36/AS<sub>1</sub>) - Hypha of *M. neogenicus* showing capitate appressoria with head cells  
1348 and stalk cells (Scale Bar = 20  $\mu$ m); (d) *Dysoxylum raptiensis* Khan et al. (2015a) from Upper  
1349 Siwalik sediments of Southeastern Himalaya (CUH/PPL/IB7/17) – SEM of the abaxial cuticle,  
1350 inner surface, paracytic stomata (Scale bar = 10  $\mu$ m); (e) Fossil leaf of *Shorea* Khan et al.  
1351 (2019b) from Middle Siwalik sediments of Bhutan (CUH/PPL/BH/12A) (Scale bar = 1 cm); (f)  
1352 Fossil fruit of *Dalbergia prelatifolia* Khan and Bera (2014) from Lower Siwalik sediments of  
1353 Darjeeling foothill (CUH/PPL/SV/f/1) (Scale bar = 1 cm); (g) Fossil fruit of *Elaeocarpus*  
1354 *prelancaefolius* Bera et al. (2004) from Upper Siwalik sediments of Southeastern Himalaya  
1355 (CUH/PPL/IB7/5/F<sub>1</sub>) (Scale bar = 1 cm); (h) Zig-zag type leaf mining on the fossil leaf of  
1356 *Terminalia panandhroensis* (Lakhanpal and Guleria) Khan et al. (2014b) from Middle Siwalik  
1357 sediments of Southeastern Himalaya (CUH/PPL/ B/54) (Scale bar = 1 cm); (i) Scanning electron

1358 micrographs of *Gmelina siwalika* Khan et al. (2018a) from Upper Siwalik sediments of  
1359 Southeastern Himalaya (CUH/PPL/C<sub>3</sub>/44) - transverse section of the secondary xylem showing  
1360 vessel with a prominent tylosis (Scale bar = 50  $\mu$ m); (j) *Dysoxylum raptiensis* Khan et al. (2015a)  
1361 from Upper Siwalik sediments of Southeastern Himalaya (CUH/PPL/IB7/17) - adaxial cuticle  
1362 with characteristic frass-trail (Scale bar = 10  $\mu$ m)

1363 **Figure 6.** (a) Diagrammatic representation of different types of forest elements of the lower  
1364 Siwalik flora of the eastern Himalayas (E = Evergreen, D = Deciduous, O = Others); (b)  
1365 Diagrammatic representation of different types of forest elements of middle Siwalik flora of the  
1366 eastern Himalayas (E = Evergreen, D = Deciduous, O = Others); (c) Diagrammatic  
1367 representation of different types of forest elements of upper Siwalik flora of the eastern  
1368 Himalayas (E = Evergreen, D = Deciduous, O = Others); (d) Diagrammatic representation of  
1369 different types of forest elements of entire Siwalik flora of the eastern Himalayas (E =  
1370 Evergreen, D = Deciduous, O = Others); (e) Schematic sketch of the floristic pattern changes  
1371 throughout the Siwalik sediments in the eastern Himalayas.

1372 **Figure 7.** Reconstruction of the palaeovegetation during Siwalik sedimentation of the eastern  
1373 Himalayas.

1374 **Figure 8.** CLAMP WorldClim2 regression models for (a) mean annual temperature (MAT) and  
1375 (b) cold month mean temperature (CMMT). The position of the eastern Himalayan fossil flora  
1376 along the second-order polynomial regression relating the MAT and CMMT vector scores for  
1377 modern vegetation against the observed MATs and CMMTs for those sites is shown as a red-  
1378 rimmed circle with a yellow center, with uncertainty bars (1 s.d.) reflecting the scatter of the  
1379 residuals about the regression line. Modern vegetation sites are coded for the climate their leaves  
1380 are adapted to, as shown in Fig. 7a. The vector score represents the relative position of the sites,

1381 modern and fossil, along with a vector representing the primary trend of the climate variable in  
1382 axes 1–4 space. See the CLAMP website (<http://clamp.ibcas.ac.cn>) for details.

1383 **Figure 9.** (a) Diagrammatic representation of Siwalik flora of the eastern Himalayas represented  
1384 in the present-day flora of different geographical regions (NE = Northeast India; SI = South  
1385 India; IM = India and Malaya Peninsula; M = Malaya; C = Cosmopolitan; O = Others); (b)  
1386 Diagrammatic representation of the Siwalik flora of the eastern Himalayas in three different  
1387 categories (EL = Extant local taxa; ELE = Extant but locally extinct taxa; ERE = extant but  
1388 regionally extinct taxa).

1389 **Figure 10.** Map showing hypothetical migratory routes of Siwalik and Southeast Asian tropical  
1390 elements.

1391

1392

1393

1394

1395

1396

1397

1398

1399

1400

1401

1402



Table 1

Group	Sub - group	Generalized Siwalik Lithology	Age			Formation		
			Darjeeling	Bhutan	Southeastern Himalaya	Darjeeling	Bhutan	Southeastern Himalaya
S I W A L I K	Upper Siwalik	Loosely packed, friable very course-grained grey sandstones with high limonitisation in places and intercalated with claystones and shales. Frequent boulder beds with a sandy matrix also occur in this formation. Remains of wood, leaves and fruits have been recorded	Pliocene	Pliocene-Pleistocene	Late Pliocene-early Pleistocene	Murti boulder bed	Formation III	Kimin Formation
	Middle Siwalik	Generally weakly indurated, medium to coarse-grained sandstones with salt and pepper texture. Calcareous concretions of various shapes and sizes occur in the sandstones, occasionally associated with grey shales with plant fossils	Late Miocene-Pliocene	Late Miocene-Pliocene	Pliocene	Parbu grit Geabdat sandstone	Formation II	Subansiri Formation
	Lower Siwalik	Well-indurated medium to fine-grained generally well-sorted sandstones, subordinate micaceous sandstones, bluish nodular silty shale, claystone, and small lenses of coal; plant fossils occur frequently	Middle Miocene	late Miocene	Late Miocene		Formation I	Dafla Formation
				Middle Miocene	Gish Clay/Chunabati formation			

Table 2

<b>FERNS</b>	<i>Homonoia mioriparia</i> Antal and Prasad (L; D)
<b>Thelypterideaceae</b>	
<i>Thelypteridaceophyllum tertiarum</i> (Joshi and Mehrotra) Khan et al. (L; SEH)	<i>Macaranga denticulate</i> Khan et al. (L; SEH)
<b>Cyatheaceae</b>	<i>M. siwalika</i> Antal and Awasthi (L; D)
<i>Cyathea Siwalika</i> Bera et al. (L; SEH)	<i>Mallotus kalimpongensis</i> Antal and Awasthi (L; D)
<b>GYMNOSPERM</b>	
<b>Pinaceae</b>	<b>Fabaceae</b>
<i>Pinus daflaensis</i> Khan and Bera (L; SEH)	<i>Acacia miocatechuoides</i> Khan and Bera (F; SEH)
<b>ANGIOSPERMS</b>	<i>Albizia palaeolebbek</i> Antal and Awasthi (L; D)
<b>Monocots</b>	<i>Albizinium arunachalensis</i> Mehrotra et al. (W; D)
<b>Marantaceae</b>	<i>Bauhinia ramthiensis</i> Antal and Awasthi (L; D)
<i>Clinogyne ovatus</i> Antal and Prasad (L; D)	<i>Bauhinium palaeomalabaricum</i> Antal et al. (L; D)
<i>C. lishensis</i> Antal and Prasad (L; D)	<i>B. siwalika</i> Khan et al. (L; SEH)
<b>Poaceae</b>	<i>Callerya precinerea</i> Khan et al. (L; SEH)
<i>Bambusa</i> sp. Antal and Awasthi (L; D)	<i>Cassinium borooahii</i> Mehrotra et al. (L; SEH)
<i>B. siwalika</i> (Joshi and Mehrotra) Khan et al. (L; SEH)	<i>Cynometra palaeoiripa</i> Prasad et al. (L; D)
<b>Arecaceae</b>	<i>C. tertiara</i> Antal and Awasthi (L; D)
<i>Amesoneuron</i> Joshi and Mehrotra (L; SEH)	<i>Cynometroxylon</i> sp. cf. <i>C. holdenii</i> Mehrotra et al. 1999 (W; D)
<b>ANGIOSPERMS</b>	<i>C. holdenii</i> Mehrotra et al. (W; D)
<b>Dicots</b>	<i>Dalbergia prelatifolia</i> Khan and Bera (F; D)
<b>Achariaceae</b>	<i>D. rimosa</i> Khan et al. (L; SEH)
<i>Gynocardia butwalensis</i> Prasad et al. (L; D)	<i>Derrisocarpon miocenicum</i> Mitra and Banerjee (F; D)
<i>G. arunachalensis</i> Khan et al. (L; SEH)	<i>Derrisophyllum siwalicum</i> Mitra and Banerjee (L; D)
<i>G. mioodorata</i> (Prasad et al.) Khan et al. (L; SEH)	
<b>Anacardiaceae</b>	
<i>Bouea premacrophylla</i> Antal and Awasthi (L; D)	
<i>Buchanania palaeosessilifolia</i> Prasad et al. (L; D)	

<i>Dracontomelum mangiferum</i> Khan et al. (L; SEH)	<i>Entada palaeoscandens</i> Antal and Awasthi (F; D)
<i>Glutoxylon burmense</i> Mehrotra et al. (W; SEH)	<i>Milletia extensa</i> Khan et al. (L; SEH)
<i>Mangifera someshwarica</i> Khan et al. (L; SEH)	<i>M. koilabasensis</i> (Prasad and Tripathi) Srivastava and Mehrotra (L; SEH, B)
<i>Nothopogia eutravancorica</i> Antal and Awasthi (L; D)	<i>M. miosericea</i> Prasad et al. (L; D)
<i>Sorindeia subansiriensis</i> Khan et al. (L; SEH)	<i>M. oodlabariensis</i> Antal and Prasad (L; D)
<b>Annonaceae</b>	<i>M. prakashii</i> Prasad et al. (L; D)
<i>Artabotrys siwalicus</i> Prasad et al. (L; D)	<i>M. purniyagiriensis</i> Prasad et al. (L; D)
<i>Cerbera miocenica</i> Prasad et al. (L; D)	<i>M. sevokensis</i> Prasad et al. (L; D)
<i>Fissistigma palaeobicolor</i> Joshi and Mehrotra (L; SEH)	<i>M. siwalika</i> Khan et al. (L; SEH)
<i>F. senii</i> Prasad et al. (L; SEH)	<i>Mastertia neoassamica</i> Khan and Bera (F; SEH)
<i>Meiogyne sevokensis</i> Prasad et al. (L; D)	<i>Pongamia siwalika</i> Antal and Awasthi Khan et al. (L; D, SEH)
<i>Mitrephora siwalika</i> (Antal and Awasthi) Prasad and Tripathi (L; D, B)	<i>P. kathgodamensis</i> Khan et al. (L; SEH)
<i>Polyalthia palaeosiamiarum</i> Antal and Prasad (L; D)	<i>Pahudioxylon bankurensis</i> Mehrotra et al. (W; D)
<i>Polyalthioxylon arunachalensis</i> Srivastava et al. (W; SEH)	<i>P. indicum</i> Srivastava et al. (W; SEH)
<i>Pseuduvaria mioreticulata</i> Prasad et al. (L; D)	<i>Spatholobus siwalicus</i> Prasad et al. (L; D)
<i>Uvaria ghishia</i> Antal and Prasad (L; D)	<b>Fagaceae</b>
<i>U. neograndiflora</i> Khan et al. (L; SEH)	<i>Quercus</i> sp. Khan et al. (L; SEH)
<i>U. siwalica</i> Prasad et al. (L; SEH)	<i>Quercus lamellosa</i> Khan et al. (L; SEH)
<b>Apocynaceae</b>	<b>Flacourtiaceae</b>
<i>Alstonia mioscholaris</i> Antal and Awasthi (L; D)	<i>Alsodeia palaeoechinocarpa</i> Antal and Prasad (L; D)
<i>Chonemorpha miocenica</i> (Prasad et al. Khan et al. (L; D, SEH)	<i>A. palaeoracemosa</i> Antal and Prasad (L; D)
	<i>A. palaeozeylanicum</i> Antal and Awasthi (L; D)
	<i>Casearia pretomentosa</i> Antal and Awasthi (L; D)
	<i>Flacourtia tertiara</i> Antal and Prasad (L; D)
	<i>Hydnocarpus palaeokurzii</i> Antal and

<i>Tabernaemontana precoronaria</i> Srivastava and Mehrotra (L; SEH)	Awasthi (L; D)
<b>Asteraceae</b>	<i>H. ghishiensis</i> Prasad et al. (L; D)
<i>Vernonia palaeoarborescens</i> Antal and Awasthi (L; D)	<b>Lamiaceae</b>
<b>Burseraceae</b>	<i>Premna plio bengalensis</i> Khan et al. (L; SEH)
<i>Bursera preserrata</i> Antal and Awasthi (L; D)	<i>Gmelina siwalika</i> Khan et al. (L; SEH)
<i>B. serratoidea</i> Antal and Awasthi (F; D)	<b>Lauraceae</b>
<i>Canarium bengalense</i> Khan et al. (L; SEH)	<i>Actinodaphne palaeoangustifolia</i> (Antal and Awasthi) Khan et al. (L; D; SEH)
<b>Calophyllaceae</b>	<i>A. palaeomalabarica</i> Srivastava and Mehrotra (L; SEH)
<i>Calophylloxydon cuddalorensis</i> Srivastava et al., (W; SEH)	<i>A. palaeoobovata</i> Khan et al. (L; SEH)
<i>C. eoinophyllum</i> Khan et al. (W; SEH)	<i>Beilschmiedia plioroxburghiana</i> Khan et al. (L; SEH)
<i>C. suraikholaensis</i> (Antal and Awasthi) Joshi and Mehrotra; Khan et al. (L; D, SEH)	<i>Cinnamomum</i> sp. Antal and Awasthi (L; D)
<i>C. siwalikum</i> Khan et al. (L; D)	<i>C. palaeobejloghota</i> Khan and Bera (L; D)
<b>Celastraceae</b>	<i>Litsea preglabrata</i> Srivastava and Mehrotra (L; SEH)
<i>Lophopetalumoxylon indicum</i> Srivastava and Mehrotra (L; SEH)	<i>L. salicifolia</i> Khan et al. (L; SEH)
<i>Salacia miocenica</i> Srivastava and Mehrotra (L; SEH)	<i>Lindera neobifaria</i> Khan and Bera (L; SEH)
<b>Clusiaceae</b>	<i>L. pulcherrima</i> Khan et al. (L; SEH)
<i>Garcinia eocambogia</i> Prasad et al. (L; D)	<i>Persea miogamblei</i> Khan and Bera (L; D)
<i>Kayexylon assamicum</i> Srivastava et al. (W; SEH)	<i>P. mioparviflora</i> Khan and Bera (L; SEH)
<b>Combretaceae</b>	<i>P. neovillosa</i> Khan and Bera (L; D)
<i>Combretum sahnii</i> (Antal and Awasthi) Khan et al. (L; D, SEH)	<i>P. preglaucescens</i> Khan and Bera (L; SEH)
<i>C. miocenicum</i> Prasad and Tripathi (L; B)	<b>Lythraceae</b>
<i>C. prechinense</i> Khan et al. (L; SEH)	<i>Lagerstroemia</i> sp. Tripathi et al. (L; B)
<i>Lagerstroemia patelii</i> Antal and Awasthi (L; D)	<i>L. jamraniensis</i> Khan et al. (L; SEH)
<i>Terminalia miobelerica</i> Antal and Prasad (L;	<i>L. deomaliensis</i> Srivastava et al. (L; SEH)
	<i>L. deomaliensis</i> Mehrotra et al. (W; SEH)
	<b>Malvaceae</b>
	<i>Bombax palaeomalabaricum</i> Prasad et al. (L; D)
	<i>Grewia ghishia</i> Antal and Awasthi (L; D)

D)	<i>G. tistaensis</i> Antal and Prasad (L; D)
<i>T. palaeocatappa</i> Joshi et al. (L; SEH)	<i>Pterospermum siwalicum</i> Antal and Prasad (L; D)
<i>T. palaeochebula</i> Khan et al. (L; SEH)	<i>P. palaeoheynianum</i> Antal and Awasthi (L; D)
<i>Terminalioxylon belericum</i> Mehrotra et al. (W; SEH)	<i>Sterculia miocolorata</i> Prasad et al. (L; D)
<b>Connaraceae</b>	<i>S. siwalica</i> Prasad et al. (L; D)
<i>Rourea miocaudata</i> Khan and Bera (L; SEH)	<i>S. mioparviflora</i> (L; D)
<b>Cornaceae</b>	<b>Melastomaceae</b>
<i>Mastixia asiatica</i> Khan et al. (F; SEH)	<i>Memecylon arunachalensis</i> Srivastava and Mehrotra (L; SEH)
<i>M. siwalika</i> Khan et al. (L; SEH)	<b>Meliaceae</b>
<b>Dilleniaceae</b>	<i>Beddomia palaeoindica</i> Antal and Prasad (L; D)
<i>Dillenia palaeoindica</i> Antal and Awasthi (L; D)	<i>Dysoxylum miocostulatum</i> Khan and Bera (L; SEH)
<b>Dipterocarpaceae</b>	<i>D. raptiensis</i> Khan et al. (L; SEH)
<i>Dipterocarpus siwalicus</i> (Prasad and Tripathi) Antal and Prasad; Joshi and Mehrotra, Khan et al. (L; B, D, SEH)	<i>Toona siwalika</i> Prasad and Tripathi (L; B)
<i>D. koilabasensis</i> Khan et al. (L; SEH)	<b>Moraceae</b>
<i>Dipterocarpoxyton parabaudii</i> Tripathi et al. (W; B)	<i>Ficus retusoides</i> Antal and Awasthi (L; D)
<i>Hopea kathgodamensis</i> Antal and Prasad (L; D)	<i>F. oodlabariensis</i> Antal and Awasthi (L; D)
<i>H. siwalika</i> Antal and Awasthi (L; D)	<i>F. precunea</i> Prasad et al. (L; D)
<i>Hopenium kalagarhensis</i> Tripathi et al. (L; B)	<b>Myristicaceae</b>
<i>Hopeoxylon speciosum</i> Mehrotra et al. (W; SEH)	<i>Knema glaucescens</i> Khan et al. (L; SEH)
<i>H. eosiamensis</i> Srivastava et al. (W, SEH)	<b>Myrtaceae</b>
<i>Shorea miocenica</i> Antal and Prasad (L; D, SEH)	<i>Syzygium palaeocuminii</i> Antal and Prasad (L; D)
<i>S. bengalensis</i> Antal and Prasad (L; D)	<b>Oleaceae</b>
<i>S. bhalukpongensis</i> Khan et al (FC; SEH)	<i>Chionanthus siwalicus</i> Prasad et al. (L; D)
<i>S. chandernagarensis</i> Khan et al (FC; SEH)	<b>Rhamnaceae</b>
	<i>Rhamnus siwalicus</i> Prasad et al. (L; D)
	<i>Ventilago tistaensis</i> Antal and Prasad (L; D)
	<i>Ziziphus palaeoapetala</i> Antal and Prasad (L; D)

<i>S. mioassamica</i> Khan and Bera (FC; SEH)	D)
<i>S. mioobtusa</i> Khan and Bera (F; A)	<b>Rubiaceae</b>
<i>S. neoassamica</i> Joshi and Mehrotra (L; SEH)	<i>Callicarpa siwalika</i> Antal and Awasthi (L; D)
<i>S. nepalensis</i> Khan et al (L; SEH)	
<i>S. palaeoridleyana</i> Joshi and Mehrotra (L; SEH)	<i>Gardenia precoronaria</i> Prasad et al (L; D)
<i>S. pinjoliensis</i> Khan and Bera (FC; SEH)	<i>Neolamarckia paleocadamba</i> Khan et al. (L; SEH)
<i>S. pliotumbugaia</i> Khan et al (L; SEH)	<i>Randia miowallichii</i> (Antal and Awasthi) Srivastava and Mehrotra (L; D, SEH)
<i>S. siwalika</i> (Antal and Awasthi) Khan et al. (L; D, SEH)	<i>R. lishensis</i> Prasad et al. (L; D)
<i>Shoreoxylon evidens</i> Mehrotra et al. (W; SEH)	<b>Rutaceae</b>
<i>Vatica siwalica</i> Prasad et al. (L; D)	<i>Toddalia miocenica</i> Prasad et al. (L; D)
<i>V. prenitida</i> Prasad et al. (L; D)	<b>Sapindaceae</b>
<b>Ebenaceae</b>	<i>Euphoria longanoides</i> Antal and Awasthi (L; D)
<i>Diospyros palaeoargentea</i> Prasad et al. (L; D)	<i>Cupania oodlabariensis</i> Prasad et al. (L; D)
<i>D. koilabasensis</i> Antal and Awasthi (L; D)	<i>Euphorioxylon deccanense</i> Mehrotra et al. (W; SEH)
<i>Ebenoxylon miocenicum</i> Antal et al. (W; D)	<i>Filicium koilabasensis</i> Prasad et al. (L; D)
<i>E. siwalicus</i> Srivastava et al. (W; SEH)	<i>Paranephelium miocenica</i> Prasad et al. (L; D)
<b>Elaeocarpaceae</b>	<i>Sabia eopaniculata</i> Prasad et al. (L; D)
<i>Elaeocarpus prelanceaefolius</i> Bera et al. (F; SEH)	<b>Vitaceae</b>
<i>Sloanea pliodasycarpa</i> More et al. (L; D)	<i>Vitis siwalicus</i> Prasad et al. (L; D)
<b>Euphorbiaceae</b>	<b>Xanthophyllaceae</b>
<i>Croton caudatus</i> Khan et al. (L; SEH)	<i>Xanthophyllum mioflavescens</i> Antal and Prasad (L; D)
<i>Dicotylophyllum breyniodes</i> Srivastava and Mehrotra (L; SEH)	
<i>Glochidion palaeohirsutum</i> Antal and Prasad (L; D)	<b>Abbreviations</b>
<i>G. siwalikum</i> Khan et al. (L. SEH)	L: Leaf; F: Fruit; W: Wood; B: Bhutan; D: Darjeeling; SEH: Southeastern Himalaya
<i>G. palaeogamblei</i> Khan et al. (L. SEH)	

**Table 3.**

<b>Locality</b>	<b>Siwalik Strata</b>	<b>Age (Formation)</b>	<b>MAT (°C)</b>	<b>WMMT (°C)</b>	<b>CMMT (°C)</b>	<b>MIN_T_W (°C)</b>	<b>MAX_T_C (°C)</b>	<b>THERM. (°C)</b>	<b>GDD_0</b>	<b>GDD_5</b>	<b>LGS (months)</b>
Darjeeling	Lower Siwalik	Middle Miocene (Gish Clay Formation)	24.2 (25.37)	28.2 (28.35)	18.7 (17.88)	22.6	24.3	602	107.9	107.2	12.8 (12.95)
Southeastern Himalaya	Upper Siwalik	Late Pliocene to early Pleistocene (Kimin Formation)	25 (25.38)	28 (28.05)	20.3 (20.86)	22.8	25.9	646	111.1	108.9	12.7 (12.58)
Southeastern Himalaya	Middle Siwalik	Pliocene (Subansiri Formation)	23.3 (23.67)	27.3 (28.14)	18.3 (16.92)	23.1	23.6	588	102	101.5	12 (12.1)
Southeastern Himalaya	Lower Siwalik	Middle Miocene (Dafla Formation)	25.2 (25.29)	28.0 (27.84)	20.7 (21.29)	22.9	26.4	653	111.4	109.1	12.7 (12.48)
Bhutan	Middle Siwalik	Late Miocene to Pliocene (Formation II)	24.3 (24.1)	27.3 (27.8)	20 (18.9)	23.1	25.4	626	106.2	104.9	12.3 (12.1)
Standard deviation			±2.4	±2.9	±3.6	±2.9	±3.5	±75	±11.7	±10.4	±1.1

Table 4.

Locality	Siwalik Strata	Age (Formation)	GSP (cm)	MMGSP (cm)	3WET (cm)	3DRY (cm)	ENTH (kJ/kg)
Darjeeling	Lower Siwalik	Middle Miocene (Gish Clay Formation)	235.3 (242.33)	21.8 (24.5)	119.1 (111.73)	24.9 (28.86)	353.3 (354.1)
Southeastern Himalaya	Upper Siwalik	Late Pliocene to early Pleistocene (Kimin Formation)	208.7 (189.86)	18 (15.87)	107.7 (101.64)	10.7 (8.97)	358.3 (356.1)
Southeastern Himalaya	Middle Siwalik	Pliocene (Subansiri Formation)	200.5 (198.12)	17.5 (17.9)	102.2 (99.41)	13.3 (13.78)	352.8 (351.3)
Southeastern Himalaya	Lower Siwalik	Middle Miocene (Dafla Formation)	198.3 (174.13)	16.5 (13.97)	101.5 (96.15)	9.1 (7.34)	358.3 (355.8)
Bhutan	Middle Siwalik	Late Miocene to Pliocene (Formation II)	189.9 (189.9)	15.8 (15.4)	97.4 (95.7)	10.2 (10.6)	356.5 (353.3)
Standard deviation			±64.3	±6.5	±40	±9.8	±8



Locality	Siwalik Strata	Age (Formation)	RH.				PD.				PET.ANN (mm)/10	PET.WAR M (mm)	PET.COLD (mm)
			ANNUAL (%)	ANNUAL (g/kg)	(hPa)	(hPa)	(hPa)	(hPa)	AUT (hPa)	(hPa)			
Darjeeling	Lower Siwalik	Middle Miocene (Gish Clay Formation)	77.2 (80.99)	14.5 (14.46)	6.5	4.5	6.2	8.8	6	137.7	127.6	85.8	
Southeastern Himalaya	Upper Siwalik	Late Pliocene to early Pleistocene (Kimin Formation)	81.3 (82.37)	15.5 (14.97)	7.6	4	7.1	11.5	5.4	148.6	133	107.8	
Southeastern Himalaya	Middle Siwalik	Pliocene (Subansiri Formation)	80 (78.84)	14.5 (14.01)	6.7	4	6.5	10.2	5.1	141.3	131.2	95.3	
Southeastern Himalaya	Lower Siwalik	Middle Miocene (Dafla Formation)	80.4 (81.15)	15.5 (14.91)	8.0	4.8	7.2	11.8	5.8	151.6	139.2	110.1	
Bhutan	Middle Siwalik	Late Miocene to Pliocene (Formation II)	81.7 (80.2)	15.2 (14.4)	7	3.6	6.8	10.9	4.9	147.5	134.6	106.5	
Standard deviation			±10.2	±1.8	±2.4	±3.5	±1.5	±4	±2	±16.2	±24.5	±13.8	

Table 5

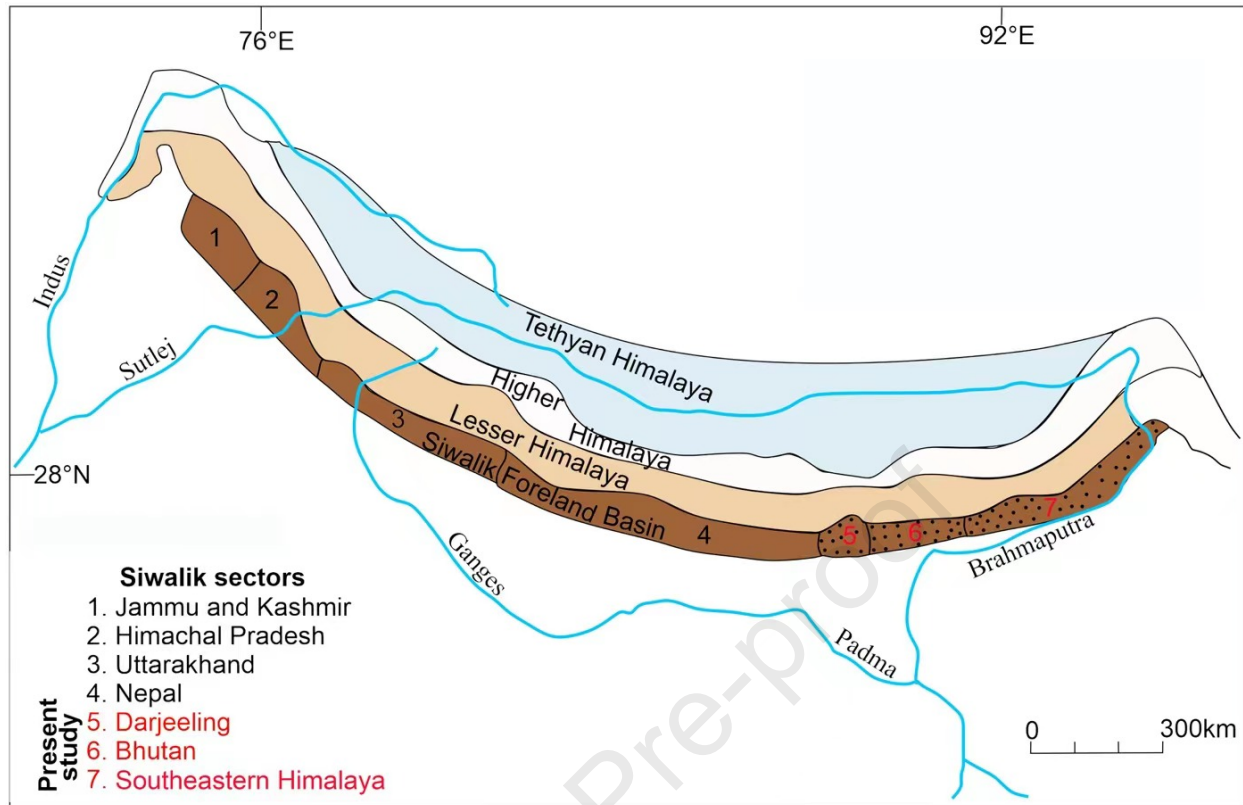


Fig. 1

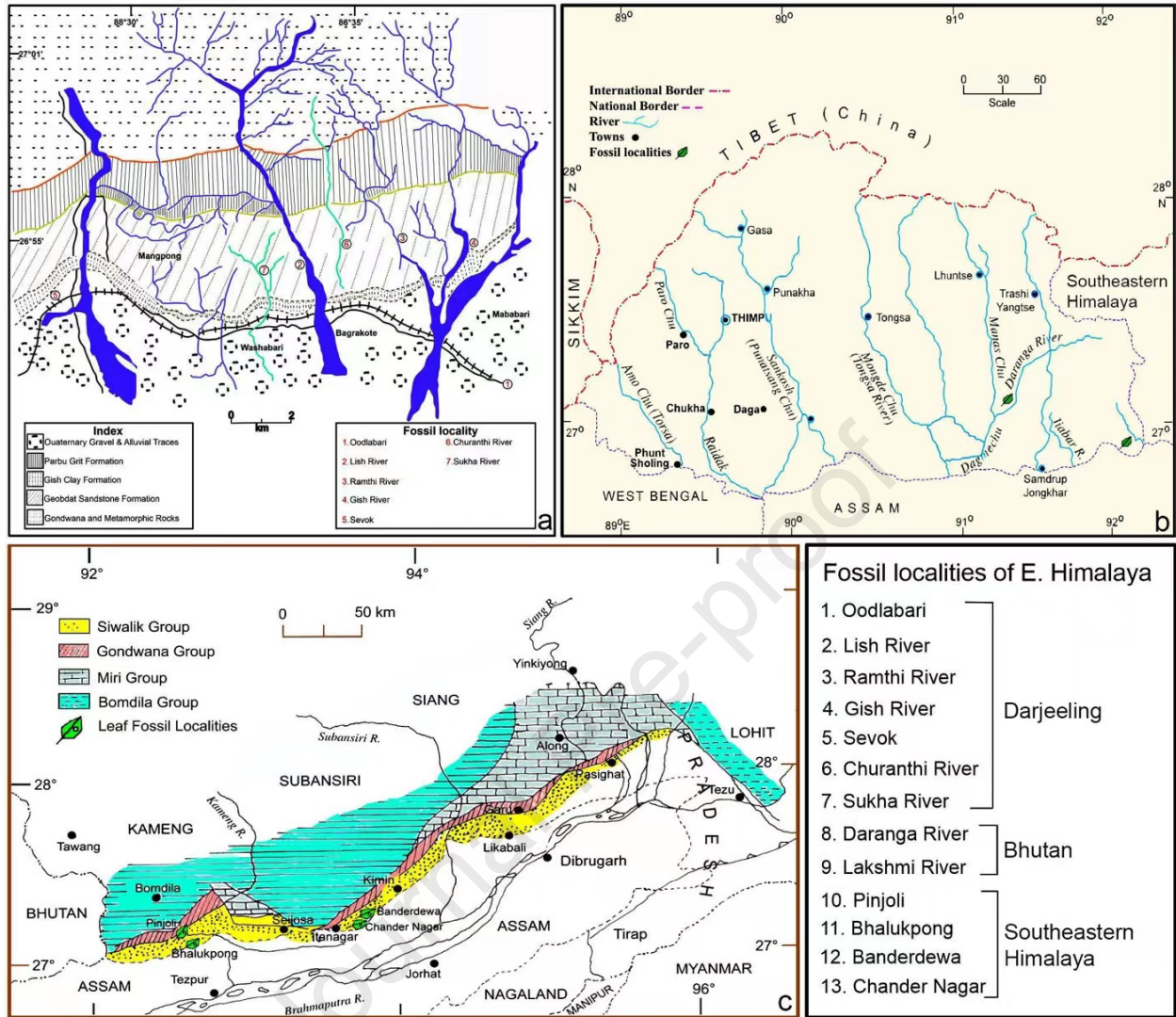


Fig. 2

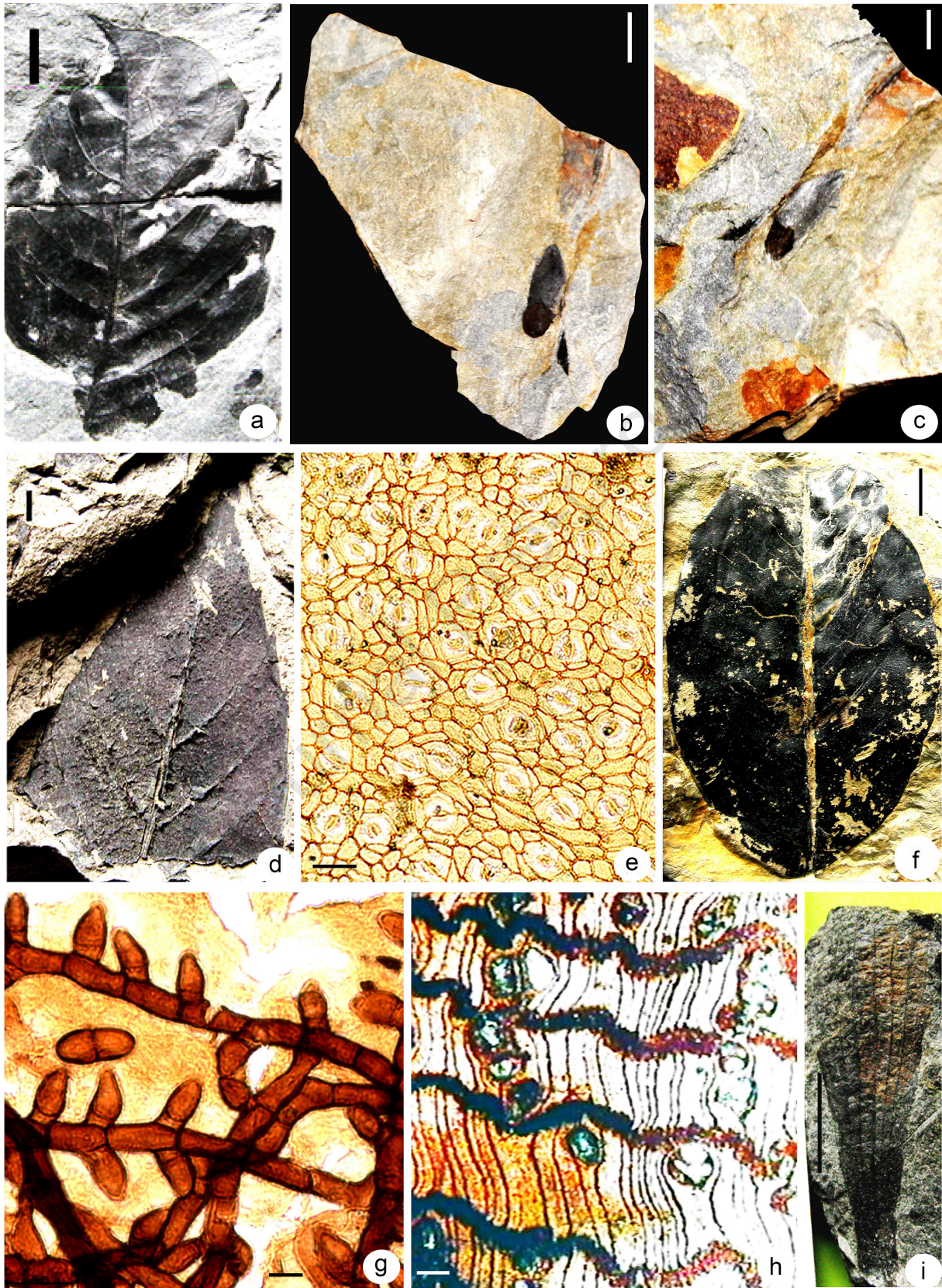


Fig. 3

Journal Pre-proof

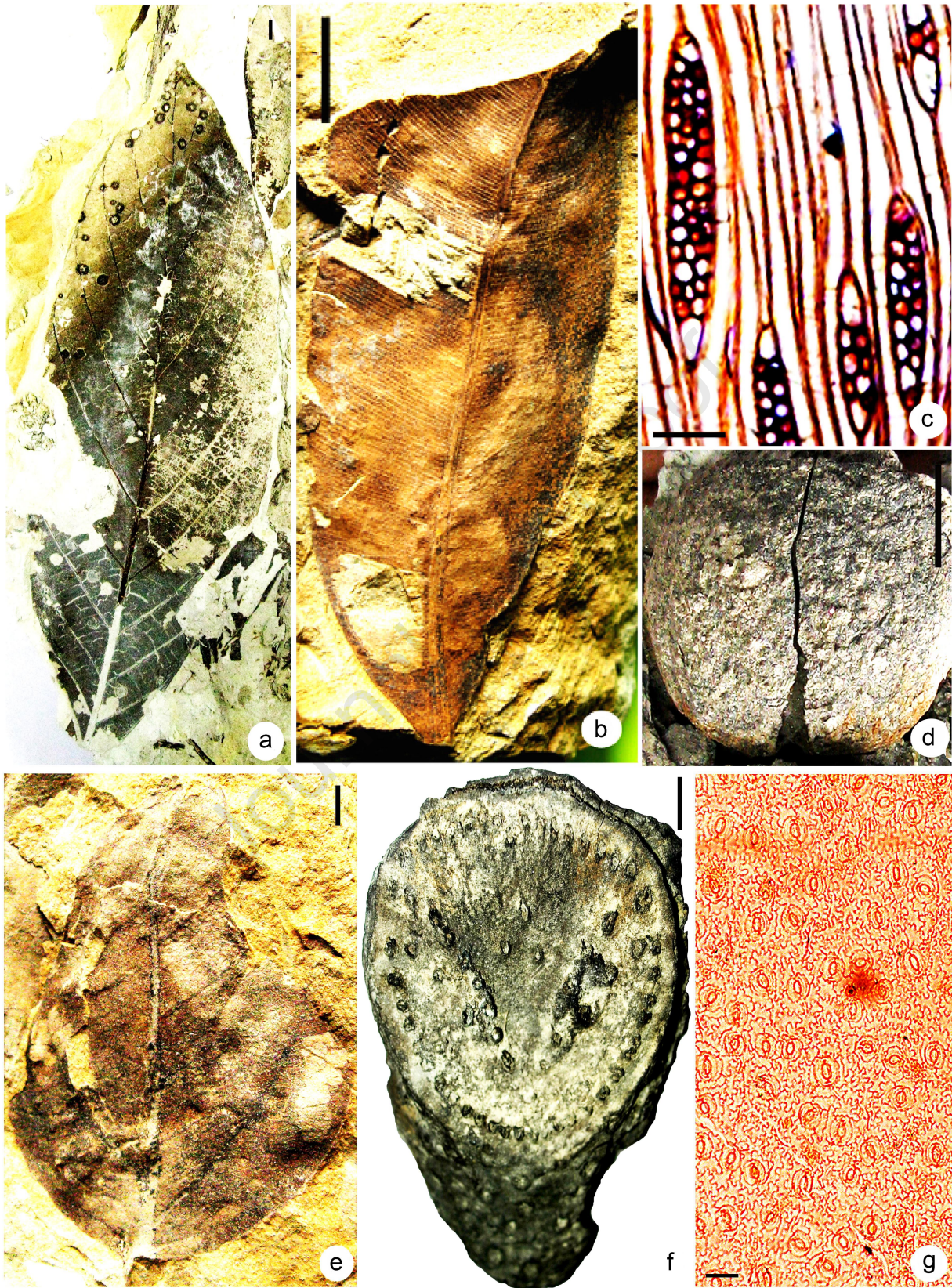


Fig. 4

Journal Pre-proof



Fig. 5



Journal Pre-proof

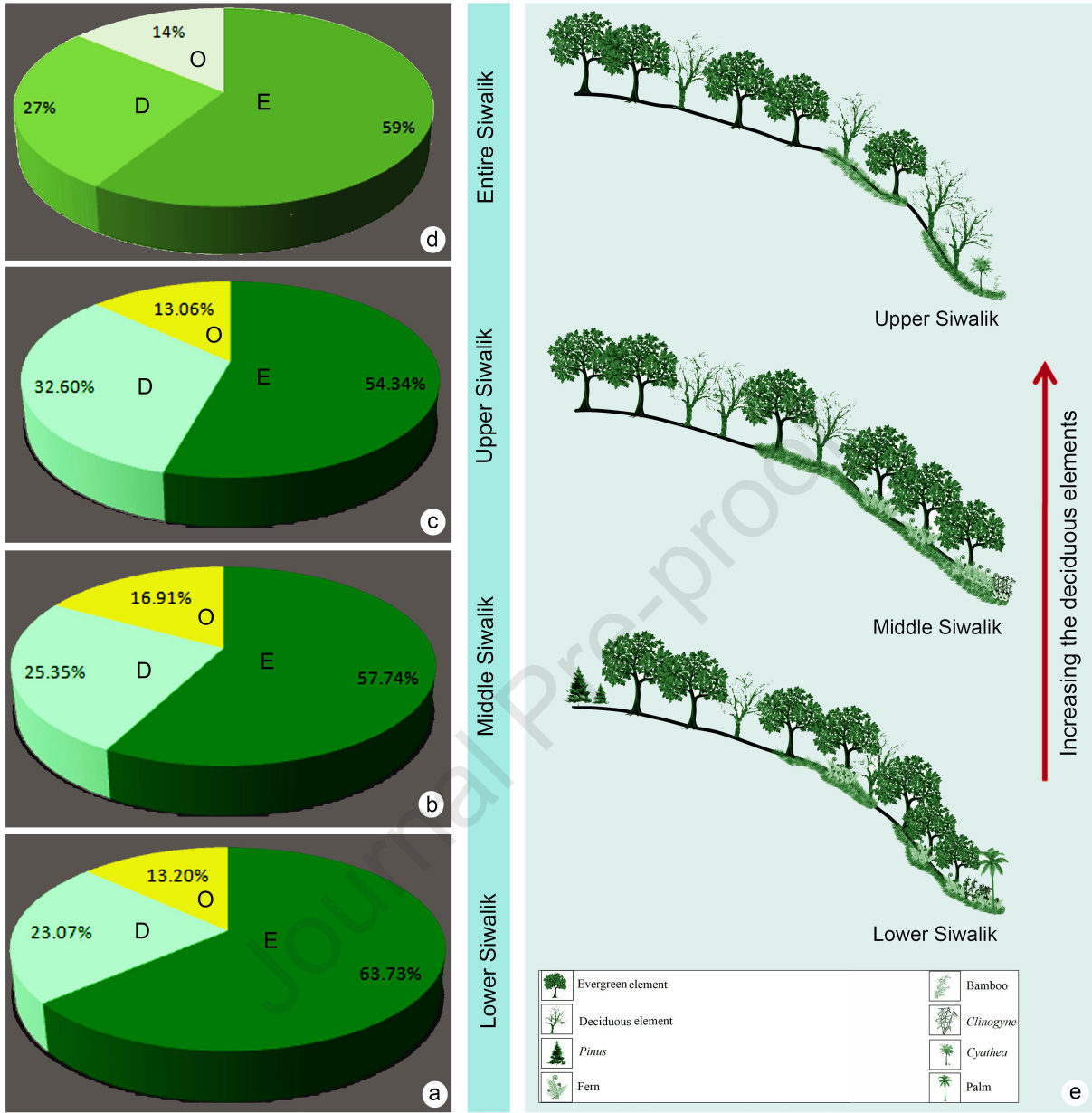


Fig. 6



Fig. 7

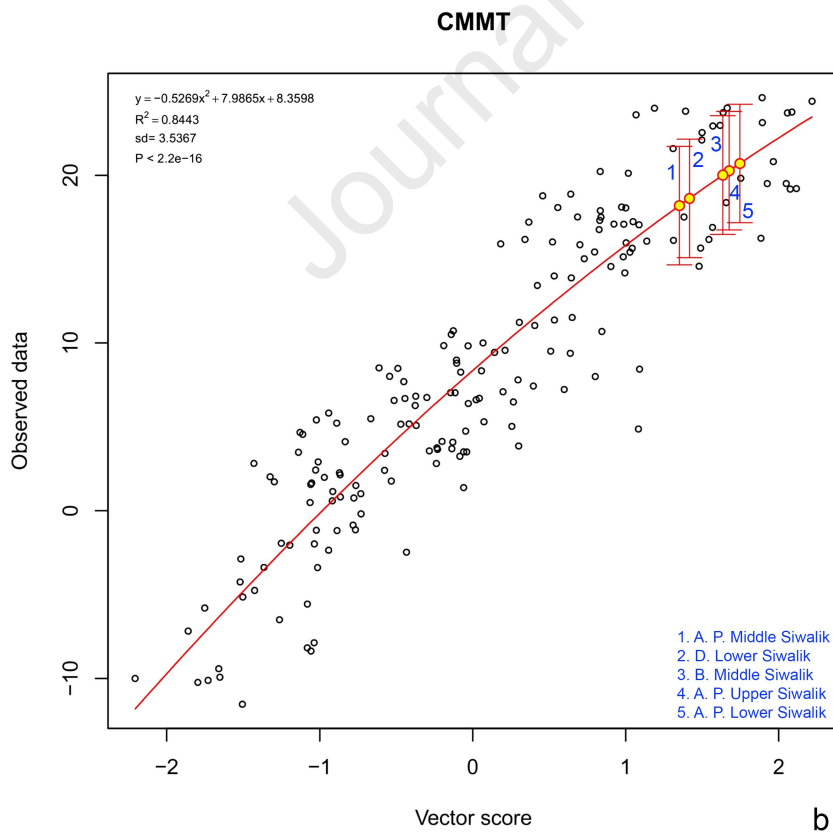
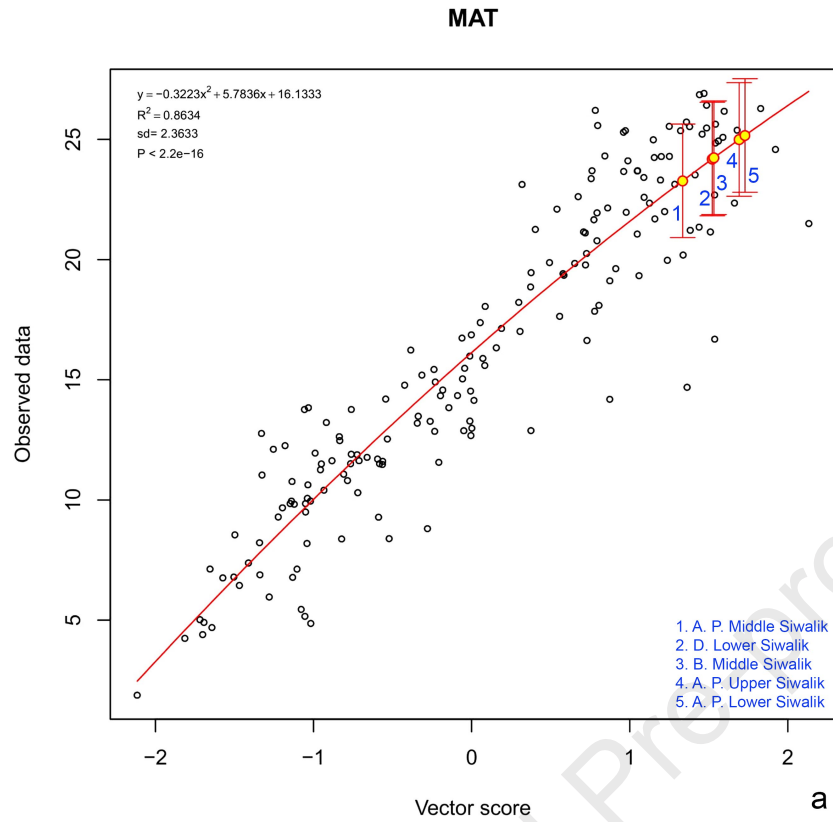


Fig. 7

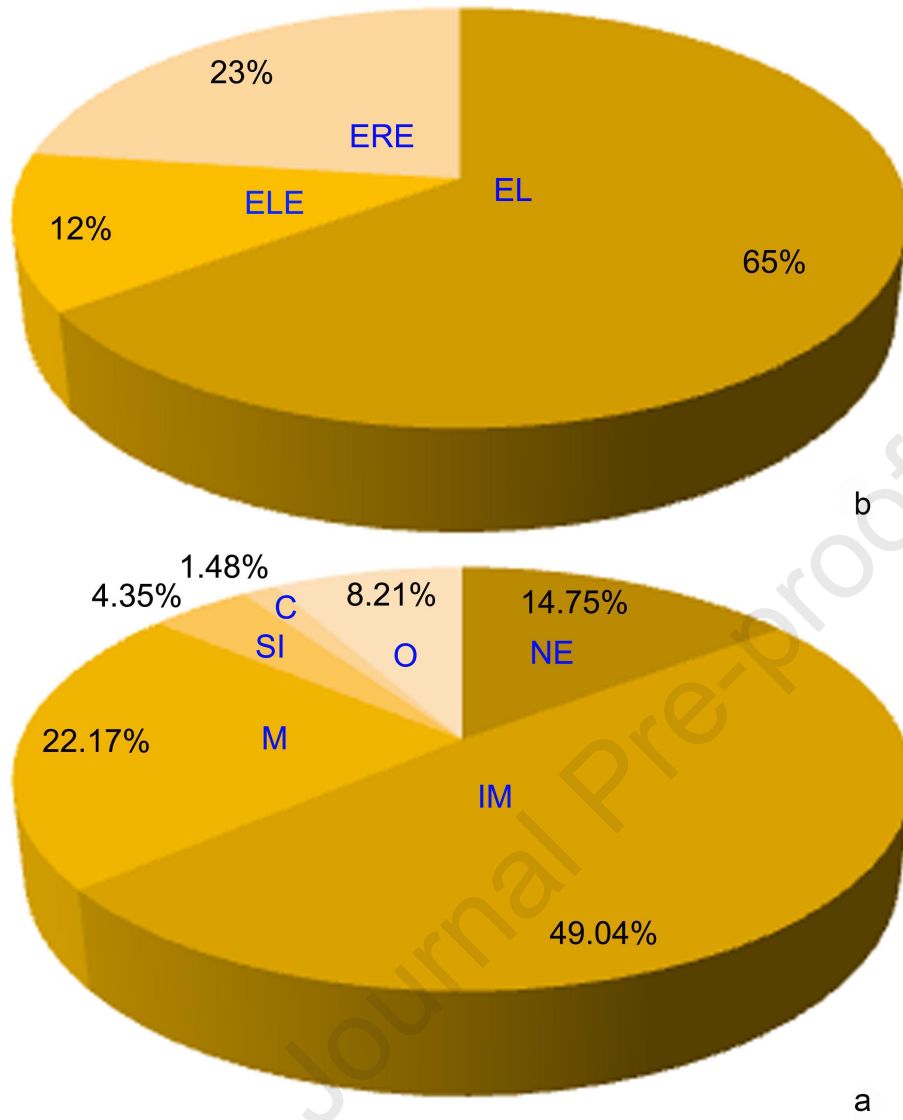


Fig. 12

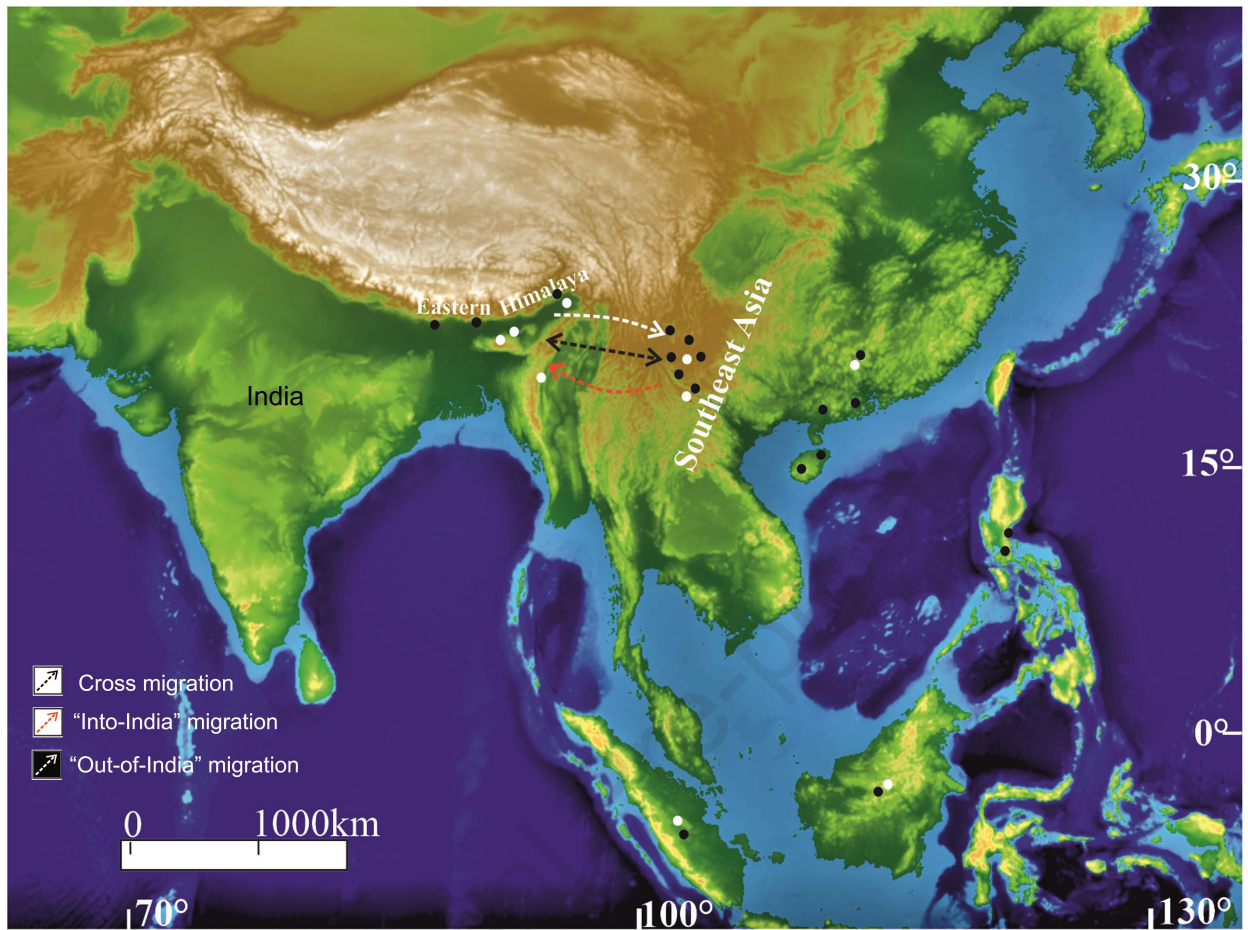


Fig. 13

### **Highlights**

- First thorough review of the eastern Himalayan Siwalik floras
- A gradual change in floral composition through the Siwalik succession
- Monsoonal tropical, warm and humid climatic conditions prevailed during the deposition
- Siwalik forests experienced a weaker monsoon (less rainfall seasonality) than now
- Phytogeographic exchanges of Siwalik elements with Southeast Asia

**The authors declare that they have no competing interests.**

Journal Pre-proof